10258 *J. Am. Chem. Soc.* **1992**, *114*, 10258-10271

$C_{30}H_{35}O_{12}N$: C, 59.89; H, 5.86; N, 2.32. Found: C, 59.71; H, 5.94; N, 2.22.

(L-**Serin-3-yl) 2,3,4,6-Tetra-*O*-acetyl-β-D-glucopyranoside (34).** Glycoside **10** (25 mg) and 5% Pd–C (25 mg) were stirred in MeOH (5 mL) under H_2 (balloon) at room temperature. After 1.5 h the Pd–C was filtered off, and the residue was evaporated to give 14 mg of **34** (98%): mp 154 °C (recrystallized from $Me_2C{=}O$); $[\alpha]^{20}{}_D = -15°$ ($c = 0.28$, MeOH); TLC R_f 0.48 (CH_2Cl_2/MeOH, 65:35); for ^1H and ^{13}C NMR data, see Tables I and II. Anal. Calcd for $C_{17}H_{25}O_{12}N$: C, 46.71; H, 5.78; N, 3.06. Found: C, 46.48; H, 5.70; N, 2.99.

[Diphenylmethyl *N*-[*N*-(*tert*-butyloxycarbonyl)-L-phenylalanyl]-L-serinate-3-yl] 2,3,4,6-Tetra-*O*-acetyl-β-D-glucopyranoside (35). Amino ester glycoside free base **33** (114 mg), HOBT (25.5 mg), and *N*-α-*t*-Boc-L-Phe (50 mg) were dissolved in dry THF (5 mL) and cooled to 0 °C, and DCCl (41 mg) was added. After the mixture was stirred overnight, the precipitate was filtered, and the solution was evaporated. The residue was dissolved in CH_2Cl_2 (50 mL), washed with saturated $NaHCO_3$ and H_2O, dried ($MgSO_4$), and chromatographed on a short column[31] (R_f 0.52 CH_2Cl_2/EtOAc, 8:2) to give 136 mg of **35** as a foam (84%): $[\alpha]^{20}{}_D = -3.1°$ ($c = 0.38$, $CHCl_3$); characteristic NMR data, ^1H NMR ($CDCl_3$) δ 7.31–7.16 (m, 15 H, aromatic H), 6.82 (s, 1 H, $CHPh_2$), 2.04–2.00 (4s, 12 H, $4O{=}CCH_3$), 1.34 (s, 9 H, $C(CH_3)_3$); ^{13}C NMR ($CDCl_3$) δ 100.71 (C1), 79.86 ($\mathit{C}(CH_3)_3$), 61.53 (C6), 28.06 ($C(\mathit{C}H_3)_3$); FAB-MS (glycerin matrix) calcd monoisotopic mass for $C_{44}H_{52}O_{15}N_2$ 848.33, *m/z* 849.25 [MH^+].

[*N*-(9-Fluorenylmethoxycarbonyl)-L-serin-3-yl] 2,3,4,6-Tetra-*O*-acetyl-β-D-glucopyranoside (36). Amino acid glycoside **34** (331 mg) was stirred in a mixture of 10% $NaHCO_3$ in water (5 mL) and dioxane (3 mL) at 0 °C. Fmoc-Cl (197 mg) in dioxane (3 mL) was added over 30 min. After stirring at 0 °C for 4 h and then at room temperature for 8 h, the reaction mixture was evaporated, dissolved in CH_2Cl_2 (60 mL), washed with H_2O (3 × 10 mL), dried, evaporated, and chromatographed[31] (R_f 0.67 CH_2Cl_2/MeOH, 8:2) to give 295 mg of **36** as a foam (92%): $[\alpha]^{20}{}_D = +25°$ ($c = 0.4$, $CHCl_3$); characteristic NMR data, ^1H NMR ($CDCl_3$) δ 7.79–7.26 (m, 8 H, aromatic H), 5.66 (bd, 1 H, NH), 4.51 (d, 1 H, H-1, $J_{1,2} = 7.1$ Hz), 3.66 (ddd, 1 H, H-5), 2.09–2.01 (4s, 12 H, $4O{=}CCH_3$). Anal. Calcd for $C_{32}H_{35}O_{14}N$: C, 58.44; H, 5.36; N, 2.12. Found: C, 58.30; H, 5.44; N, 2.01.

H_2N-Tyr-D-Cys-Gly-Phe-D-Cys-Ser(*O*-β-D-Glc)-Gly-$CONH_2$ (38). Peptide assembly via Fmoc chemistry was performed manually (0.85-g scale, 10-mL wash volumes), starting with 4-[[(2′,4′-dimethoxyphenyl)(9-fluorenylmethoxycarbonyl)amino]methyl]phenoxy resin (Rink's[18a] resin, Bachem California) (0.46 mmol/g). Fmoc removal was accomplished with piperidine/DMF (3:7, 3 × 10 min), followed by washing with DMF (6 × 1 min). Couplings were achieved by adding the reagents sequentially to the resin in the following order: 1.5 equiv of Fmoc amino acid, 1.5 equiv of BOP reagent, 1.5 equiv of HOBT, and 2.5 equiv of $i Pr_2NEt$. The mixture was agitated by bubbling argon through the reaction mixture (frit) for 1–2 h (negative ninhydrin test obtained). Upon completion of chain assembly, the Fmoc group was removed as above. The acetyl protecting groups for the glucoside moiety were removed with $H_2NNH_2 \cdot H_2O$/MeOH (4:1, 2 h) while the peptide remained anchored to the resin. The excess H_2NNH_2 was washed with MeOH (4 × 1 min) and CH_2Cl_2 (4 × 1 min). The cleavage was carried out with $CF_3COOH/CH_2Cl_2/H_2O$ (8:16:1, 100 mL), which also removed the *tert*-butyl ether from the side chain of the tyrosine. The filtrate was diluted with H_2O (100 mL) and vacuum distilled at 25 °C to a volume of 100 mL. After lyophilization, the crude glycopeptide was dissolved in water (20 mL), the acidity was adjusted to pH 4 with AcOH, and $Hg(OAc)_2$ (140 mg) was added. After stirring for 75 min, the reaction was diluted with H_2O (180 mL) and treated with H_2S. The HgS precipitate was removed by filtration, and excess H_2S was purged with a stream of N_2. The peptide was oxidized with aqueous $K_3Fe(CN)_6$ (312 mg in 1000 mL of H_2O) while the acidity was kept constant (pH 8.4) with NH_4OH. After 10 h the acidity was adjusted to pH 4 with AcOH, Amberlite 68 resin (Cl^- form) was added, and the reaction was stirred until the yellow color disappeared. After filtration the reaction was lyophilized and purified by HPLC ($t_R = 24.9$ min, 0–50% MeCN in 0.1% aqueous TFA in 50 min, C_{18} column) to provide enkephalin analogue **38** in 28% yield based on resin: characteristic ^1H NMR data, ^1H NMR (D_2O) δ 7.33–7.23 (m, 5 H, Phe aromatic H), 7.12, 6.84 (dd, 4 H, Tyr aromatic H), 4.40 (d, 1 H, H-1, $J_{1,2} = 7.8$ Hz); FAB-MS (glycerol matrix) calcd monoisotopic mass for $C_{37}H_{50}O_{14}N_8S_2$ 894.28, *m/z* 895.56 [MH^+].

Acknowledgment. We thank the University of Arizona for a Biomedical Research Support Grant (BRSG No. S07RR07002), the University of Arizona Foundation, the American Cancer Society for an Institutional Cancer Research Grant Award, and the National Science Foundation (CHE-9201112). Acknowledgement is made to the donors of the Petroleum Research Fund, administered by the American Chemical Society (ACS-PRF No. 21005-G7), and to a National Institute of Drug Abuse Grant (DA 06284) for partial support of this research.

Investigation of the Modes of Solubilization and Norrish II Photoreactivity of 2- and *sym*-*n*-Alkanones in the Solid Phases of *n*-Heneicosane and Two Homologues[1]

Alberto Nuñez,[†] George S. Hammond, and Richard G. Weiss*

Contribution from the Department of Chemistry, Georgetown University, Washington, D.C. 20057.

Received April 6, 1992

Abstract: The nature of the solubilization sites and the solubility limits of a homologous series of 2- and *sym*-*n*-alkanones (**2-*N*** and ***m*-*N***, respectively) have been investigated in the hexagonally and orthorhombically packed layered solid phases of heneicosane (**C21**) by differential scanning calorimetry, deuterium magnetic resonance, and optical microscopy. The photoselectivity and relative quantum efficiencies of product formation from the alkanones in the same solid phases were determined. Results from experiments employing the solid phases of eicosane (**C20**) and hexacosane (**C26**) were also obtained. The data show that the solid phases of *n*-alkanes impose severe restrictions on the motions of the alkanones and their photochemically-generated hydroxy-1,4-biradical intermediates only when the solutes fit well within a solvent layer. In those cases, extremely large photoselectivities, larger than those from analogous smectic liquid-crystalline phases, can be achieved. However, the ability of a solid *n*-alkane phase to incorporate an alkanone of a different length is much more limited than in the smectic phases. Eutectic mixtures and phase-separated alkanone crystals are obtained in many of the systems investigated.

Introduction

The mechanistic features of Norrish Type II photoreactions of *n*-alkanones (eq 1) have been studied extensively and are well understood.[2] In isotropic media, quantum yields are rather insensitive to variations in temperature and solvent viscosity; the

---

[†] Present address: Department of Chemistry, Temple University, Philadelphia, PA 19122.

(1) Liquid-Crystalline Solvents as Mechanistic Probes. 47. Part 46: Vilalta, P. M.; Weiss, R. G. *Liq. Cryst.* **1992**, *12*, 531.

0002-7863/92/1514-10258$03.00/0

ratio of elimination to cyclization products (*E*/*C*) varies only within rather narrow limits, and the trans/cis ratios (*t*/*c*) of diasteromeric cyclobutanols change substantially with solvent polarity[3] but not with temperature[3,4] or ketone chain length.[4] Since the product ratios are relatively constant under isotropic conditions, we have used Type II reactions as probes for unusual environmental influences when the ketones are guests dissolved in ordered hosts which include liquid-crystals, smectic E-like solid phases, and smectic B-like gels.[5-8] Some large deviations of the product ratios from the isotropic norms were attributed to restriction of conformational interconversion of the biradical (BR) intermediates involved in the photoreactions.

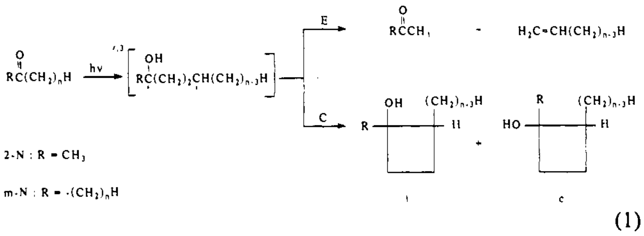

(1)

Interpretation of results from these earlier studies is complicated by the fact that the organized host molecules contain polar functional groups either at chain ends (carboxylate anions) or along the chains (ester carboxyl groups). In fact, dipolar or hydrogen-bonding interactions between a BR and polar groups of its host neighbors may be more important energetically than the steric constraints imposed by the bulk anisotropy. We now report results obtained from irradiation of *n*-alkanones in the solid layered phases of long-chain *n*-alkanes.[9] In these media, restriction of motion in the BR can be attributed only to attractive binding by dispersion forces and repulsion due to steric hindrance. The solvent used in most experiments was heneicosane ($C_{21}H_{44}$ = **C21**) although comparisons are also made with reactions in eicosane ($C_{20}H_{42}$ = **C20**) and hexacosane ($C_{26}H_{54}$ = **C26**). All of the ketones contain unbranched carbon chains and are identified as **2-*N*** or ***m*-*N***, where *N* is the number of carbon atoms and 2 or $m = (N + 1)/2$ specifies the position of the carbonyl group. Each of the systems studied, containing only a hydrocarbon and a ketone, was irradiated at temperatures above the solid–liquid transition temperature of the host and, in most cases, at two lower temperatures. Products were analyzed by gas–liquid-phase chromatography (glpc). Differential scanning calorimetry (DSC), optical microscopy, and ^{2}H NMR spectroscopy were used to characterize the physical state of the various systems and the mobility of the methylene groups in the proximity of the carbonyl groups.

Table I. Sources and Melting Points of **2-*N*** and ***m*-*N***

N	source	mp (°C) obsd	mp (°C) lit
	2-*N*		
13	Eastman	29.5–30.5	27.6[c]
15	*a*	38–39	38.9[c]
17	*b*	48.5–49	48.2[c]
18	*b*	50–51	52[c]
19	*b*	56–56.5	55.6[c]
20	*b*	59–60	59.1[c]
21	*b*	62–62.5	62.5[c]
22	*b*	64.5–65.5	64.2–65.7[d]
23	*b*	67–69	65.9–67.2[d]
25	*b*	71–72	
27	*b*	75.5–76.5	
	m*-*N		
13	Aldrich	31–32	30–31[e]
15	Aldrich	42.5–43	41.0–42.0[e]
17	Aldrich	51–51.5	52.0–53.0[e]
19	Aldrich	56–57	58.0–59.0[e]
21	Lancaster	63.5–64.5	61.5–62.0[f]
25	Lancaster	72.5	71.0–72.0[e]
27	Wiley Organics	76–77	78.0–79.0[e]
31	TCI	82–83	82–83[g]
3-heptadecanone	*b*	49–50	47.6–48.9[h]
4-heptadecanone	*b*	42.5–43	41.5–42.2[h]

[a] Gift of Dr. R. L. Treanor. [b] Synthesized as described in text. [c] Ref 28b. [d] Baykut, F.; Ozeris, S. *Istanbul Univ. Fen Fak Mecm, Serí C* **1956**, *21*, 102; *Chem. Abstr.* **1957**, *51*, 5691f. [e] Briese, R. R.; McElvain, S. M. *J. Am. Chem. Soc.* **1933**, *55*, 1697. [f] Schill, G.; Jones, P. R. *Synthesis* **1974**, *6*, 117. [g] Komae, H.; Hayashi, N. *Phytochemistry* **1971**, *10*, 1953. [h] Oldham, J. W. A.; Ubbeholde, A. R. *Trans. Faraday Soc.* **1939**, *35*, 328.

Experimental Section

Instrumentation. Gas–liquid-phase chromatography (glpc) was performed on a Hewlett-Packard 5890A gas chromatograph equipped with a flame ionization detector and a Hewlett-Packard 3393A integrator. Alltech RSL-300 and Chrompak (CP9Sil-19CD fused-silica open-tubular columns (0.53 mm × 10 m) were employed. NMR spectra were recorded on a Bruker AM-300 WB spectrometer with an Aspect 3000 computer. A CP-MAS probe (1024 FID data points) was used to record ^{2}H spectra of neat 2-, 3-, and 4-heptadecanone and of 9-heptadecanone in its eutectic mixtures with **C21**; a 10-mm multinuclear probe (8192 FID data points) was used for all other spectra. Melting points (uncorrected) and some transition temperatures were measured on a Kofler hot-stage microscope equipped with crossed polars. The radiation source for photolyses was a Hanovia 450-W medium-pressure Hg lamp with Pyrex and water filters.

Materials. Ketones were recrystallized repeatedly or passed through a silica gel column (8/3 hexane/benzene as eluent) until they were >97% pure as determined by glpc; Table I). Except as noted, all of the 2-alkanones were synthesized from the corresponding acids.[10] The 3- and 4-heptadecanones were synthesized from the corresponding alcohols (Lancaster Synthesis) by a Jones oxidation.[11a]

Deuteriation at the positions α to the carbonyl groups of **2-*N*** and ***m*-*N*** was effected by dissolving 30 mg of each ketone in ca. 2 mL of dried monoglyme (Aldrich, 99%) and refluxing the solution with 0.6 mL of D_2O and 20 mg of Na_2CO_3 in a dry atmosphere for 48 h.[11b] Deuterium incorporation α to the carbonyl groups was always >90%.

Recrystallization from acetone yielded eicosane (Aldrich), mp 37.5–38.0 °C (lit.[12] mp 36.6 °C), that was >99.9% pure by glpc analysis. Heneicosane (Humphrey) was recrystallized five times from 95/5 ethanol/hexane to yield mp 41.5–42.0 °C (lit.[12] mp 40.2 °C) and >99.5% purity by glpc. Hexacosane (Humphrey) exhibited mp 57.5–58.0 °C (lit.[12] mp 56.3 °C) and 99% purity by glpc after recrystallization from 7/3 (v/v) acetone/hexane.

Irradiation Procedures. Solutions of 1 wt% ketone (unless noted otherwise) in isotropic-phase alkane were prepared under a N_2 atmo-

---

(2) (a) Wagner, P. J. *Acc. Chem. Res.* **1983**, *16*, 461. (b) Turro, N. J.; Dalton, J. C.; Dawes, K.; Farrington, G.; Hautala, R.; Morton, D.; Niemazyk, M.; Schore, N. *Acc. Chem. Res.* **1972**, *5*, 92. (c) Wagner, P.; Park, B.-S. In *Organic Photochemistry*; Padwa, A., Ed.; Marcel Dekker: New York, 1991; Vol. 11, Chapter 4. (d) Yang, N. C.; Yang, D.-H. *J. Am. Chem. Soc.* **1958**, *80*, 2913.

(3) Zimmerman, R. G.; Liu, J. H.; Weiss, R. G. *J. Am. Chem. Soc.* **1986**, *108*, 5264.

(4) (a) Harley, G. H.; Guillet, J. E. *Macromolecules* **1968**, *1*, 413. (b) Encina, M. V.; Lissi, E. A. *J. Photochem.* **1976**, *5*, 287. (c) Encina, M. V.; Lissi, E. A. *J. Photochem.* **1975**, *4*, 321.

(5) (a) Hrovat, D. A.; Liu, J. H.; Turro, N. J.; Weiss, R. G. *J. Am. Chem. Soc.* **1984**, *106*, 7033. (b) Nerbonne, J. M.; Weiss, R. G. *Isr. J. Chem.* **1979**, *18*, 266. (c) Vilalta, P. M.; Hammond, G. S.; Weiss, R. G. *Photochem. Photobiol.* **1991**, *54*, 563.

(6) (a) Treanor, R. L.; Weiss, R. G. *Tetrahedron* **1987**, *43*, 1371. (b) He, Z.; Weiss, R. G. *J. Am. Chem. Soc.* **1990**, *112*, 5535. (c) Weiss, R. G.; Treanor, R. L.; Nuñez, A. *Pure Appl. Chem.* **1988**, *60*, 999.

(7) Treanor, R. L.; Weiss, R. G. *J. Am. Chem. Soc.* **1988**, *110*, 2170.

(8) Treanor, R. L. Ph.D. Thesis, Georgetown University, Washington, DC, 1987.

(9) For preliminary accounts, see: (a) Nuñez, A.; Weiss, R. G. *J. Am. Chem. Soc.* **1987**, *109*, 6215. (b) Nuñez, A.; Weiss, R. G. *Bol. Soc. Chil. Quim.* **1990**, *35*, 3.

(10) Jorgenson, M. J. *Organic Reactions*; Bittman, R., Dauben, W. G., Fried, J., House, H. O., Kende, A. S., Marshall, J. A., McKusick, B. C., Meinwald, J., Eds.; Wiley: New York, 1970; Vol. 18, Chapter 1.

(11) (a) Wiberg, K. B. In *Oxidation in Organic Chemistry*; Wiberg, K. B., Ed.; Academic Press: New York, 1965; Chapter II. (b) Trost, B. M.; House, H. O. *J. Org. Chem.* **1965**, *30*, 1341.

(12) Schaerer, A. A.; Busso, C. J.; Smith, A. E.; Skinner, L. B. *J. Am. Chem. Soc.* **1955**, *77*, 2017.

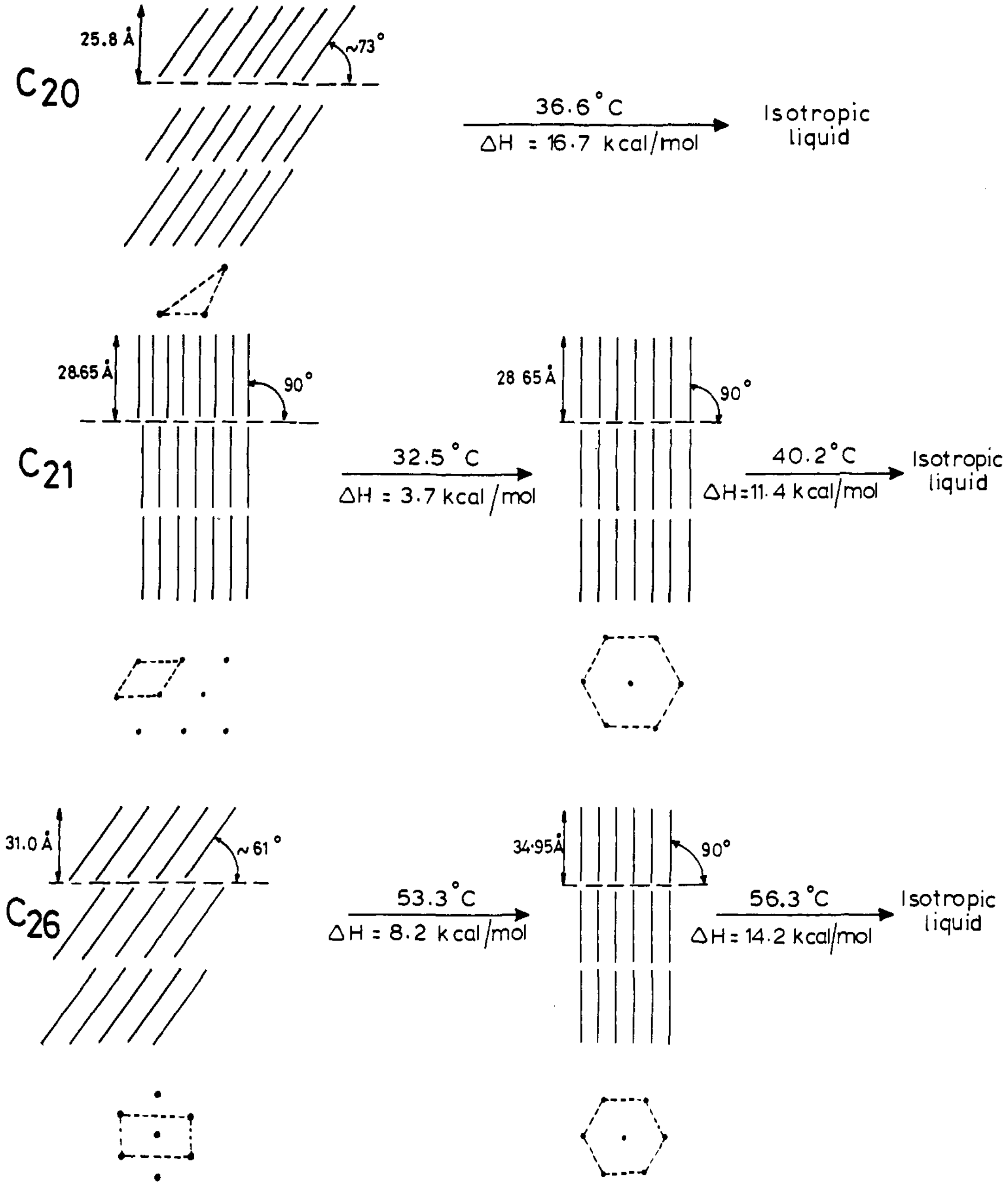

Figure 1. Representation of the packing arrangements of the solid phases of **C20**, **C21**, and **C26**.[14]

sphere. Approximately equal aliquots were transferred under N_2 to Pyrex capillary tubes (0.8–1.1-mm i.d.) that were flame-sealed. The tubes were heated until the solution became isotropic and were then incubated in a Haake temperature bath (±0.5 °C) for 30 min prior to irradiation. Longer incubation periods did not alter the photochemical results. The lamp jacket was placed in the thermostating bath, and irradiations of several tubes were conducted for empirically determined periods to allow desired percent conversions to be attained.

The *t*/*c* ratios were calculated in some cases from samples irradiated to ca. 65% conversion. Ratios from experiments at lower and higher percent conversions of ketone usually agreed within the limits of the precision errors. *E*/*C* ratios were calculated from irradiations with <15% conversion. At low conversions, only the Norrish II photoproducts could be detected by glpc. Assignment of peaks from *cis*- and *trans*-cyclobutanols and from alkene elimination products was made as described previously.[5,6–9] Truncated alkanone elimination products were identified via coinjection with authentic samples. Product ratios are not corrected for differences in detector responses.

For determination of relative quantum yields (Φ_{rel}), three (or more) sealed capillary tubes containing equal weight aliquots of 3.25×10^{-5} mol/g ratio samples of **m-N** (0.7–1.5 wt% depending upon ketone length) in heneicosane were incubated as before and irradiated in a merry-go-round apparatus through a mask that exposed equal areas of each tube to the light. In order to normalize the Φ_{rel} among the various ketones, at least one tube containing 11-heneicosanone in heneicosane was irradiated alongside the other tubes to serve as a standard. Irradiations at different temperatures for one ketone were conducted on the same day to minimize changes in lamp intensity. However, duplicate irradiations conducted on different days led to results that agreed within the precision limits shown in Table II.

DSC Thermograms. A Perkin-Elmer DSC-2 with an intercooler or a Dupont 1090B thermal analyzer with a Model 910 cell base was employed to measure heat flows and transition temperatures in samples. Usually, 4–6 mg of an alkane containing some **2-N** or **m-N** was sealed in a two-piece aluminum pan assembly. Heating cycles to 10–25-deg above the melting point of the higher melting component were recorded at a heating rate of ≤2.5 deg/min. Duplicate runs showed very small deviations in ΔH (<1 cal/g) and temperatures of maximum heat flow (<0.5 °C using the Dupont instrument and <1 °C using the Perkin-Elmer instrument).

^{2}H NMR Spectra. Samples of 3 wt% **2-N** or **m-N** (unless stated otherwise) in heneicosane were equilibrated in the spectrometer probe at the desired temperature for 45–60 min prior to the commencement of FID collection or were incubated for 8 h outside the magnet at 39 °C prior to being placed rapidly in the probe (preheated to 39 °C). Usually, the intensity of singlets (relative to quadrupolar doublets) decreased during the first 20 min after cooling a sample. The quadrupole-echo pulse sequence[13] with full phase cycling was employed. Typically,

Table II. Relative Quantum Yields (Φ_{rel}) for Disappearance of 3.25 × 10^{-5} mol/g of ***m*-*N*** in **C21**

N	$h\nu$ time (min)	*T* (°C)	% conversion[a]	Φ_{rel}
13	60	45	12 ± 2	0.5 ± 0.1
	60	35	15 ± 3	0.7 ± 0.2
	60	25	22 ± 4	1.0 ± 0.2
21	50	45	11 ± 2	0.6 ± 0.1
	50	35	11 ± 3	0.6 ± 0.2
	90	25	7 ± 3	0.2 ± 0.1
27	50	45	12 ± 2	0.6 ± 0.1
	240	35	14 ± 2	0.15 ± 0.01
	60	25	10 ± 1	0.6 ± 0.1
31	50	45	11 ± 2	0.6 ± 0.1
	630	35	5 ± 2	0.03 ± 0.01
	120	25	7 ± 3	0.2 ± 0.1

[a] One standard deviation from the average of three samples with three injections per sample. The percent of consumed starting ketone is reported.

3000-6000 scan accumulations gave sufficient signal-to-noise ratios for analysis.

Results

Solid *n*-Alkane Phases (Figure 1). There are two solid phases of **C21**: Phase I below 32.5 °C and Phase II between 32.5 and 40.2 °C,[14,15] the transition temperature to the isotropic phase. Molecules in Phase II are fully extended and arranged in hexagonally packed layers, described as a "rotator" phase. The long axes of the molecules are normal to the layer planes,[14] as in smectic B liquid-crystals,[16] and the individual molecules can execute complicated rotational jumps and form transitory gauche defects primarily concentrated in chain segments lying close to the layer interfaces.[15,17] In Phase I, the molecules are orthorhombically packed,[15] as in smectic E liquid-crystals.[16] Molecular rotations are damped and there are very few deviations from all-trans conformations.

Eicosane exists in a rigid triclinic solid phase in which the long molecular axes are fully extended in all-trans conformations and are inclined at a non-normal angle with respect to the layer planes,[14] as in smectic G and H phases.[16] Methylene groups near the center of a triclinic layer are even more rigidly constrained than those in an orthorhombic phase.[17b] Hexacosane exists as a monoclinic solid below 53.3 °C and as a rotator phase from 53.3 to 56.3 °C.[14] In general, layers of even-numbered *n*-alkanes pack more closely than do those of the odd-numbered ones.[17f]

Thermal Measurements. DSC and optical microscopy were used to assess the state of the various two-component systems. Hysteresis is common to all samples on cooling. At concentrations below 3 wt% of all of the ketones, except **16-31** and those with *N* = 13 and 27, no heating endotherms which could not be assigned to **C21** were evident. Furthermore, microscopic observations gave little or no indication of anomalous behavior; the apparent heats of fusion and melting temperatures, T_m, deviated slightly from those of neat **C21** in some cases. Since 3 wt% of both *N* = 21 ketones produced no detectable modification of the behavior of **C21**, we believe that they are accommodated in the Phase I and Phase II crystalline matrices by essentially isomorphous substitution. Relevant data are summarized in Table III.

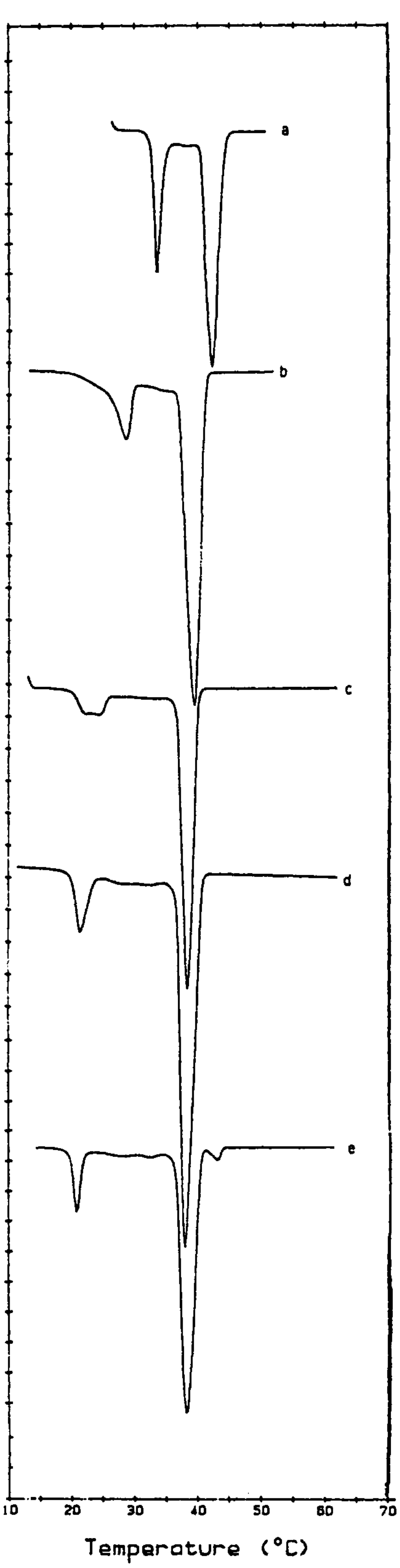

Figure 2. DSC heating thermograms (2 deg/min) of **C21** containing (a) 0, (b) 10, (c) 20, (d) 25, and (e) 30 wt% of **10-19**. Weights of samples differ so that peak areas among samples are not normalized. Heat flow per gram of sample remains constant within experimental error for all of the samples in the region of T_m.

Thermograms recorded with samples containing higher concentrations of a ketone show unmistakable nonideal solution behavior which varies considerably among the various guest molecules. Up to 15 wt% of the *N* = 21 and **2-20** ketones or up to 10 wt% of **2-22** effects very little change in the **C21** thermograms.

---

(13) Davis, J. H.; Jeffrey, K. P.; Bloom, M.; Valic, M. I.; Higgs, T. P. *Chem. Phys. Lett.* **1976**, *42*, 390.

(14) (a) Broadhurst, M. G. *J. Res. Natl. Bur. Stand.* **1962**, *66A* (3), 241 and references cited therein. (b) Small, D. M. *The Physical Chemistry of Lipids*; Plenum: New York, 1986; Chapter 7. (c) Sirota, E. B.; King, H. E., Jr.; Hughes, G. J.; Wan, W. K. *Phys. Rev. Lett.* **1992**, *68*, 492.

(15) Maroncelli, M.; Ping Qi, S.; Snyder, R. G.; Strauss, H. L. *J. Am. Chem. Soc.* **1982**, *104*, 6237.

(16) Gray, G. W.; Goodby, J. W. G. *Smectic Liquid Crystals*; Leonard Hill: Glasgow, Scotland, 1984.

(17) (a) Kelusky, E. C.; Smith, I. C. P.; Elliger, C. A.; Cameron, D. G. *J. Am. Chem. Soc.* **1984**, *106*, 2267. (b) Okazaki, M.; Toriyama, K. *J. Phys. Chem.* **1989**, *93*, 2883. (c) Brown, M. S.; Grant, D. M.; Horton, W. J.; Mayne, C. L.; Evans, G. T. *J. Am. Chem. Soc.* **1985**, *107*, 6698. (d) Maroncelli, M.; Strauss, H. L.; Snyder, R. G. *J. Chem. Phys.* **1985**, *82*, 2811. (e) Craievich, A. F.; Denicolo, I.; Doucet, J. *Phys. Rev. B* **1984**, *30*, 4782. (f) Craievich, A. F.; Doucet, J.; Denicolo, I. *Phys. Rev. B* **1985**, *32*, 4164.

Table III. Transition Enthalpies and Temperatures (Maximum Heat Flow) for 3 wt% of **2-*N*** or ***m*-*N*** in **C21**[a,b]

	2-*N*					*m*-*N*				
N	ΔH_a (cal/g)	ΔH_m (cal/g)	T_a (°C)	T_m[d] (°C)		ΔH_a (cal/g)	ΔH_m (cal/g)	T_a (°C)	T_m[d] (°C)	
13	15.7	37.8	31.4	38.9		18.1	38.0	31.5	38.7	
	(1.3)		(22.4)			(2.1)		(24.4)		
15	15.8	40.7	32.5	39.9	[30.5–38.0]	18.2	39.3	32.6	39.7	[31.0–39.0]
17	12.1	39.3	32.7	40.5	[34.5–39.0]	11.9	36.5	32.7	40.3	[33.5–38.0]
18	9.9	37.4	31.0	39.9	[35.0–38.5]					
19	10.3	37.2	29.9	39.4	[36.5–38.5]	10.5	36.2	30.2	39.0	[36.5–38.0]
20	12.7	37.8	31.2	40.0	[38.0–38.5]					
21	13.4	35.2	32.6	40.4	[38.5–39.0]	13.4	35.2	32.4	40.3	[38.0–39.0]
22	8.7	38.2	30.4	40.4	[38.5–39.0]					
23	7.1	36.5	25.5	40.1	[38.5–40.0]	9.3	37.3	28.7	40.3	[38.5–39.0]
25	8.2	39.3	28.8	40.1		10.4	36.7	27.8	39.2	[38.5–58.0]
27	6.4[c]	36.4[c]	25.6[c]	40.3[c]		4.8	31.9	26.8	41.1	
	(8.0)		(35.8)		[38.0–55.0][e]	(1.7)		(32.1)		
31						8.8	36.0	28.5	40.7	[39.0–66.0]

[a] For heneicosane: ΔH_a = 13.85 cal/g, ΔH_m = 38.85 cal/g, T_a = 32.6 °C, and T_m = 40.2 °C (lit.[14] ΔH_a = 12.47 cal/g, ΔH_m = 38.44 cal/g, T_a = 32.5 °C, and T_m = 40.2 °C). [b] Additional endotherm and its temperature of maximum heat flow are in parenthesis. [c] Average from two different samples. [d] Optically determined (uncorrected) melting point ranges in brackets from second melting of 10 wt% ketone in **C21** samples. The melting range of neat **C21** was 39.0–39.5 °C. [e] From first melting.

At higher concentrations, the samples appear to be mixtures of a solid solution of the ketone in hydrocarbon and a second phase which is mostly, perhaps almost entirely, solid ketone.

Samples of **C21** containing >3 wt% of all ketones with 23 < *N* < 19 show a variety of deviations from ideal behavior. However, *the effects of pairs of isomeric odd-numbered ketones are remarkably similar in all cases.* The tendency of the ketones to be accommodated in the hydrocarbon phases seem to be determined almost exclusively by chain length,[14b,c] with no significant sensitivity to the position of the carbonyl groups in the molecule.

The intriguing behavior of **10-19** at 10–30 wt% in **C21** is shown in Figure 2. Similar comportment is found in **2-19/C21** samples. Apparently, Phase II is formed from the melt with nearly ideal incorporation of the ketone. There is very little heat flow in the region of the Phase I–Phase II transition, but endotherms are seen at lower temperatures at all concentrations. As the concentration of the ketone is increased, the total heat flow becomes markedly less than the heat of fusion of **10-19** (54.0 cal/g) or the sum of the two transition enthalpies of heneicosane (52.7 cal/g).[14] With 30 wt% of **10–19**, the total exothermicity is 44.0 cal/g. We conclude that even the 30 wt% solid sample contains little, if any, phase-separated ketone.

In one model to account for these and other observations on cooling, isotropic liquid solution containing ca. 25 wt% of **10-19** ketone, when cooled through T_m of C_{21}, solidifies to the Phase II structure without great disordering while dissolved ketone is accommodated as a solute. As the sample is brought to below the Phase I–Phase II transition temperature, the ketone "holds" the solid in the Phase II structure in which it obviously can be included much more comfortably than in a Phase I molecular arrangement.[14b,c] At 21 °C, phase separation almost certainly occurs. One of the phases is probably Phase I hydrocarbon with a small amount of ketone dissolved in it. The other phase, probably a eutectic,[18] contains both ketone and hydrocarbon. Eutectics have been identified in solid mixtures of longer *n*-alkanes, also.[18b] Separation of the same solid phases can be detected in samples containing less than the eutectic amount of ketone.

Thermograms with 3 wt% of both *N* = 17 ketones contain broad heat flow maxima at 32 and 40 °C, suggesting that both Phase I and Phase II are formed but that the solute ketones create considerable disorder in the hydrocarbon lattices. At 10 wt%, both heptadecanones depress T_m of **C21** slightly (to 39 °C), and new heat flow maxima at 35.5–36 and 29.5 °C appear (Figure 3). At 30 wt%, the higher temperature maxima disappear entirely while the 35.7 °C transition becomes very strong.

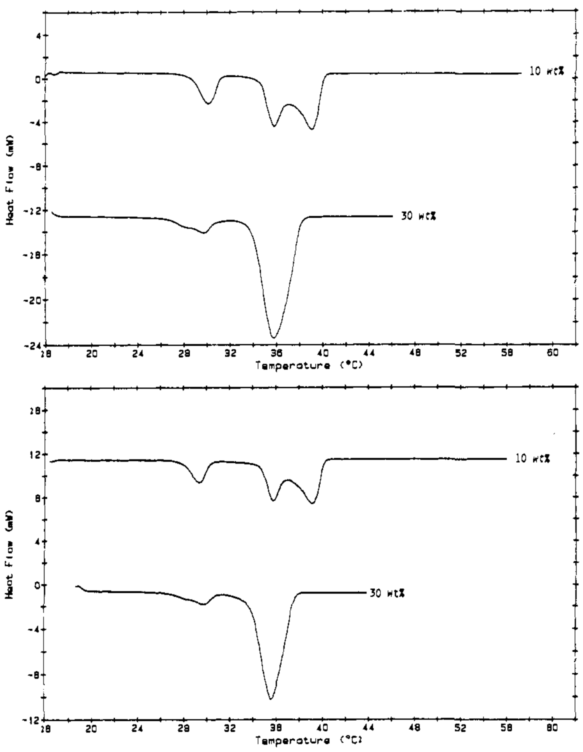

Figure 3. DSC heating thermograms (2 deg/min) of **C21** containing (a, top) 10 and 30 wt% of **2-17** and (b, bottom) 10 and 30 wt% of **9-17**.

The ^{2}H NMR spectra of deuteriated ketones in these systems are those of essentially pure ketones (vide infra). We presume that, at 30 wt% of heptadecanone, a *eutectic mixture*,[18] consisting of nearly pure ketone microcrystals mixed with **C21** microcrystals, is formed at 35.5–36 °C. The transformation occurring below 30 °C indicates the formation of some Phase I hydrocarbon, perhaps containing some dissolved ketone, as well as an uncharacterized transition. At 30 wt%, the aggregate enthalpies of melting are equal (±5%) to the value expected for the sum of the two solids independently; the enthalpy of melting of neat **2-17** is 55.7 cal/g. The overall result is quite reasonable because of the contribution to the total free energy of fusion of the entropy of mixing of the two species in the isotropic liquid.

Heating thermograms of samples with 3 and 10 wt% *N* = 13 ketones in **C21** show three maxima. The endotherm at highest temperature remains near 38.7 °C in the 3 wt% samples and is shifted to slightly lower temperature at 10 wt%. Another endotherm occurs very close to 31.5 °C in all cases, and a third is

---

(18) (a) Adamson, A. W. *A Textbook of Physical Chemistry*, 3rd ed.; Academic Press: New York, 1986; pp 400 ff. (b) Dorset, D. L. *Macromolecules*, **1990**, *23*, 623.

Table IV. Transition Enthalpies and Temperatures (Maximum Heat Flow) for 3 wt% of **2-*N*** and ***m*-*N*** in **C20** and **C26**[a]

		2-*N*			***m*-*N***		
solvent	N	ΔH_m (cal/g)	$\Delta T_m{}^d$		ΔH_m (cal/g)	$T_m{}^d$ (°C)	
C20[b]	17	57.2 (3.3)	36.1 (32.4)	[31.0–34.5]	54.5 (4.7)	36.1 (31.8)	[31.5–34.0]
C20	19	60.3	35.3	[34.5–35.0]	57.4	35.5	[31.5–34.0]
C20	20	55.1	35.3	[35.0–35.5]			
C20	21	38.7 (18.9)	35.9 (33.4)	[34.0–35.5]	40.6 (18.4)	36.0 (33.5)	[34.0–35.5]
	23						[34.5–55.5]

		2-*N*				***m*-*N***			
solvent	N	ΔH_a (cal/g)	ΔH_m (cal/g)	T_a (°C)	T_m (°C)	ΔH_a (cal/g)	ΔH_m (cal/g)	T_a (°C)	T_m (°C)
C26[c]	21	22.3 (1.6)	38.2	51.7 (47.6)	55.9	26.1 (0.3)	36.2	52.2 (47.9)	56.2
C26	27	13.0 (6.6)	40.6	50.9 (49.6)	56.6	16.4 (2.4)	38.2	51.4 (49.6)	56.5

[a] Additional endotherms and their temperatures of maximum heat flow are in parentheses. [b] ΔH_m = 58.8 cal/g and T_m = 36.0 °C (lit.[14] ΔH_m = 59.1 cal/g and T_m = 32.6 °C). [c] ΔH_a = 21.2 cal/g, ΔH_m = 37.8 cal/g, T_a = 52.1 °C, and T_m = 56.0 °C (lit.[14] ΔH_a = 21.0 cal/g, ΔH_m = 38.7 cal/g, T_a = 53.3 °C, and T_m = 56.3 °C). [d] Optically determined (uncorrected) melting point ranges in brackets from second melting of 10 wt% ketone in **C20** samples. The melting range of neat **C20** was 35.0–35.5 °C.

at 22.5 ± 0.2 °C for **2-13** and at 24.5 ± 0.1 °C for **7-13**. In spite of the near constancy of the temperatures of the endotherms, there is some shift of heat flow from the one of highest temperature to the lower ones as the solute concentrations are increased. We suggest that, (1) below 36–38 °C, the liquid solution solidifies to form a solid solution of ketone in Phase II of **C21**; (2) below 31.5 °C, separation of the solid produces Phase I hydrocarbon and a ketone-rich phase; and (3) below 22.5 or 24.5 °C, separation of the ketone-rich material occurs, probably producing pure ketone and additional Phase I hydrocarbon. It is noteworthy that the total indicated heat of transition in each case is slightly greater than the sum of the transition enthalpies of the host.

Thermograms of samples with up to 15 wt% of $N = 27$ ketones in **C21** show a broadened hydrocarbon melting transition at about 40 °C whose positions are not very reproducible (perhaps due to incomplete equilibration of the sample during heating). Samples containing 10 wt% of ketone also display a small endotherm at higher temperatures, probably from melting or dissolution of a ketone-rich phase which separates visually from the solid solution at lower temperatures; the heat of fusion of neat **14-27** is 57.4 cal/g. In most of the thermograms, there are small endothermic maxima near 35 °C and sharp ones near 26–31 °C. The maxima at lowest temperature appear at increasingly higher temperatures as the concentration of the ketones is *increased*; the heat flow associated with the transition *decreases* with increasing ketone content. At ≤3 wt% of ketone in Phase II hydrocarbon, solid solutions are formed but exist over very narrow temperature ranges. We have insufficient evidence to draw even tentative conclusions as to changes occurring in lower temperature transitions. However, by analogy with mixtures of alkane homologues, the transitions may involve restacking of molecular layers[14b] and conceivably the formation of liquid crystal-like phases.[14c]

The calorimetric behavior of a number of ketones in **C20** was examined (Table IV). Thermograms of samples containing 3 wt% of the $N = 19$ ketones or **2-20** show T_m and ΔH_m values which are indistinguishable (within experimental error) from those of the host. At 10 wt% of either $N = 19$ ketone or at 3 wt% of the $N = 17$ ketones, a second endotherm at about 32 °C appears. In these cases, there is clearly a phase separation at temperatures close to 32 °C which must reflect the presence of a ketone-rich or eutectic phase.

The thermal behavior of the samples of the $N = 21$ ketones in **C20** is somewhat strange and strongly reminiscent of that of the $N = 19$ ketones in **C21**. At 3 wt% loading, new endotherms at 33.5 °C appear; at 10 wt%, the melting transition is still present and the lower temperature transition is shifted to 22.5 °C. Furthermore, the total heat flow in the 10 wt% samples is drastically reduced. Eutectic compounds may be forming again.[18]

The pairs of isomeric $N = 21$ and $N = 27$ ketones were studied in **C26** at 3 and 10 wt% concentrations (Table IV). At 3 wt%, T_m of the host is not appreciably depressed by any of the ketones and the apparent enthalpies of melting are close to that of neat **C26**.[14a] The monoclinic-rotator solid-state transition is very slightly depressed in temperature and corresponding heat flow increases in the 10 wt% samples. We suggest that, at low loading of the ketones, monoclinic hydrocarbon may be separating from a solid solution of the ketone in the rotator phase of **C26** and, at slightly lower temperatures, a solid solution of ketone in hydrocarbon may be formed.[14b,c]

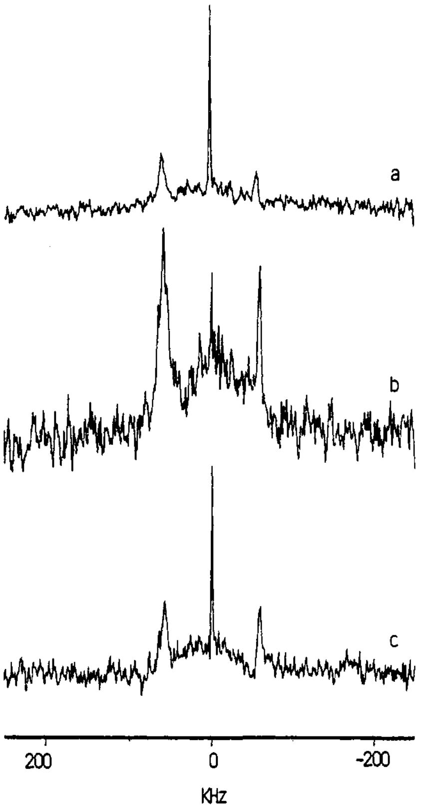

Figure 4. ^{2}H NMR spectra (10-s delay) of α-deuteriated **9-17**: (a) neat at 25 °C; (b) 30 wt% in **C21** at 25 °C; (c) 30 wt% in **C21** at 34 °C.

^{2}H NMR Spectra of Alkanones in C21. At 25 °C and 10-s delay between scans, the solid-state ^{2}H NMR spectrum of neat α-deuteriated **9-17** consists of a characteristic doublet ($\Delta\nu$ = 117.6 KHz) symmetrically disposed with respect to a small "isotropic" singlet (Figure 4). α-Deuteriated **10-19** and **11-21** afford spectra almost identical to that of **9-17** when delays are ≥10 s. The magnitude of the splittings are near the theoretical maximum for

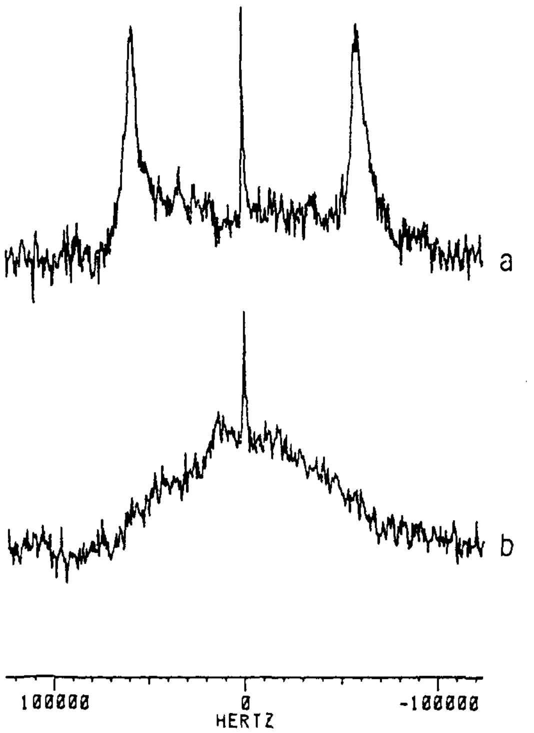

Figure 5. ^{2}H NMR spectra of α-deuteriated **11-21**: (a) neat, 30-s delay, 24 °C; (b) 12 wt% in **C21**, 10-s delay, 36 °C.

a fully extended polymethylene chain which is arranged in a layered environment and which experiences hindered rotation about its long axis.[19]

The spectrum of the same sample of neat **9-17** at the same temperature, but with a 0.5-s delay between scans, shows only the narrow singlet which arises from motionally-averaged deuterons on the small mole fraction of molecules which reside at defect sites or perhaps at crystalline surfaces. In fact, except for the very short ***m*-*N*** like **7-13** and **8-15** (which do not appear to form solid solutions in **C21** even at very low concentrations and remain liquid at lower temperatures), the deuteron resonances from the vast majority of *sym*-alkanone molecules in dilute (3 wt%) solid samples of **C21** are not detected when delay times are short, probably because of a combination of very long relaxation times and insufficient radiation power.[19a] At 25 °C (ca. 10-deg below the eutectic melting temperature), a 30 wt% sample of **9-17** in **C21** exhibits $\Delta\nu$ = 117.3 KHz. The near identity between this and $\Delta\nu$ of the neat solid ketone is proof that the eutectic is a mixture of microcrystallites of **9-17** and **C21** rather than a compound of them.[18]

The $\Delta\nu$ value of neat solid α-deuteriated **11-21** (24 °C) is 116.4 KHz. At 12 wt% (below its solubility limit) in **C21** and ca. 36 °C, only a broad hump, centered about the minor "isotropic" singlet, could be detected (Figure 5). Thus, a symmetrical alkanone that is well-incorporated into the layers of **C21** molecules behaves as though it is in a solid solution (rather than a phase-separated solid environment).

Figure 6 is a synopsis of the ^{2}H NMR spectra of samples of 3 wt% of the α-deuteriated **2-*N*** homologs in **C21** (1-s delay). The isotropic phase spectra consist solely of a narrow singlet. The magnitudes of the doublet splittings vary from ca. 16 KHz in Phase II to ca. 20 KHz in Phase I for most of the **2-*N***. At these short time delays between scans, we believe that the methyl deuterons are being detected in all of the samples and the methylene deuterons are included in only selected samples where the **2-*N*** molecules have a large disturbing influence on their local **C21** environment but do not phase separate from it as a solid.[19a] In this regard, we find that spectra of 3 wt% of **3-17** and **4-17** deuteriated α to the carbonyl groups in **C21**, taken under the same instrumental conditions as those for a sample with **2-17**, consist of a singlet and quadrupolar split signals above 25 °C. In previous studies, we have found that the mobility of methylene groups of a solute molecule imbedded in a layered phase depends upon their location within the layer *and* their position with respect to a disturbing functional group along the solute chain.[6a,b] On this basis, we suspect that deuterons at position 4 of **3-17** and at position 5 of **4-17** contribute very little to the observed quadrupolar doublets.

The data in Figure 6 follow a clear trend that is consistent with the DSC results. The spectra of **2-15** provide evidence that its α-deuterons are in a highly disordered environment, even when the **C21** solvent is macroscopically in Phase I. The Phase I derived spectra of **2-17**, **2-19**, and **2-21** evolve in their appearance; the deuterons of **2-17** appear to reside in a much more disordered environment than those of **2-21**. The longer 1,1,1,3,3-pentadeuterio **2-25** and **2-27** with an odd number of carbon atoms provide ^{2}H NMR spectra indicative of a very different deuteron environment in which much of the ketone is solid and phase-separated at 30 °C but dissolves at least partially at higher temperatures. The ^{2}H NMR spectra of **2-*N*** with an even number of carbon atoms seem to evolve also; the homogeneity of the deuteron environments increases from **2-18** to **2-22**. However, the control imposed by solid **C21** over the motions necessary to convert these 2-alkanones (at 1 wt% concentrations) to their Norrish II photoproducts is most severe with **2-20** (vide infra).

At 35 °C, the magnitudes of the most important doublet deuteron splittings decrease regularly with increasing 2-alkanone chain length (Figure 7). Each $\Delta\nu$ value relates only to the deuteron environment for that fraction of **2-*N*** which is *dissolved* in Phase II of **C21**. The data suggest that the acetyl end of the 2-alkanone molecules does not reside at the boundary of a **C21** layer when the ketone has fewer than 21 carbon atoms; Figure 8a as opposed to Figure 8b.

The relatively small $\Delta\nu$ values of **2-25** and **2-27** indicate that their deuteriated carbon atoms reside in a locally disturbed region in solid **C21**. Since these **2-*N*** will find it very difficult to remain "kinked" within one **C21** layer (Figure 8c),[20] placing the acetyl end along a layer boundary (the region of greatest entropy; Figure 8d) may be their best compromise. An alternative solubilization mode (Figure 8e) is rejected on the basis of observations that establish the reluctance of long ***m*-*N*** to span a potassium stearate/1-octadecanol (KSO) bilayer.[7] Models somewhat similar to those shown in Figure 8 have been advanced to explain data obtained with mixtures of *n*-alkanes.[14,17,20]

Spectra (1-s delay) of eutectic and neat samples of α-deuteriated **2-17** at 33 °C, slightly below the eutectic transition temperature, exhibit Pake patterns with very similar shapes and splitting parameters (Figure 9): $\Delta\nu_{90}$ = 33.5 KHz (eutectic) and 33.6 KHz (neat). Thus, **2-17** in the eutectic exists as microcrystallites[18] (like **9-17**). The additional splitting in the eutectic sample ($\Delta\nu$ = 19.5 KHz) may be from the fraction of ketone that has dissolved into the **C21** matrix. A spectrum of the eutectic mixture at 32 °C, collected with a 30-s delay between scans, showed the Pake pattern ($\Delta\nu_{90}$ = 34.0 KHz) and central singlet as before and an additional weak doublet ($\Delta\nu$ = 115.7 KHz) that can be attributed to resonances from deuterons at the 3 position of **2-17**.

Photochemistry. The influence of environments provided by solid *n*-alkanes on the photochemistry of the alkanones has been deduced from relative quantum yields (Φ_{rel}) and, in larger part, from distributions of photoproducts. Absolute quantum yields are very difficult to measure accurately in solid phases because light scattering makes precise definition of the optical path impossible. For similar reasons, small differences between numbers in Table II should not be considered mechanistically important. With a few notable exceptions, the Φ_{rel} values are 0.6 ± 0.1 of that formed for **7-13** at 25 °C.

---

(19) (a) Fyfe, C. A. *Solid State NMR for Chemists*; CFC Press: Guelph, Ontario, 1983; Chapter 3. (b) Smith, I. C. P. *NMR of Newly Accessible Nuclei*; Lazlo, P., Ed.; Academic Press: New York, 1983; Vol. 2, Chapter 1. (c) Griffin, R. G. *Methods Enzymol., Lipids* **1981**, *72*, 109.

(20) Maroncelli, M.; Strauss, H. L.; Snyder, R. G. *J. Phys. Chem.* **1985**, *89*, 5260 and references cited therein.

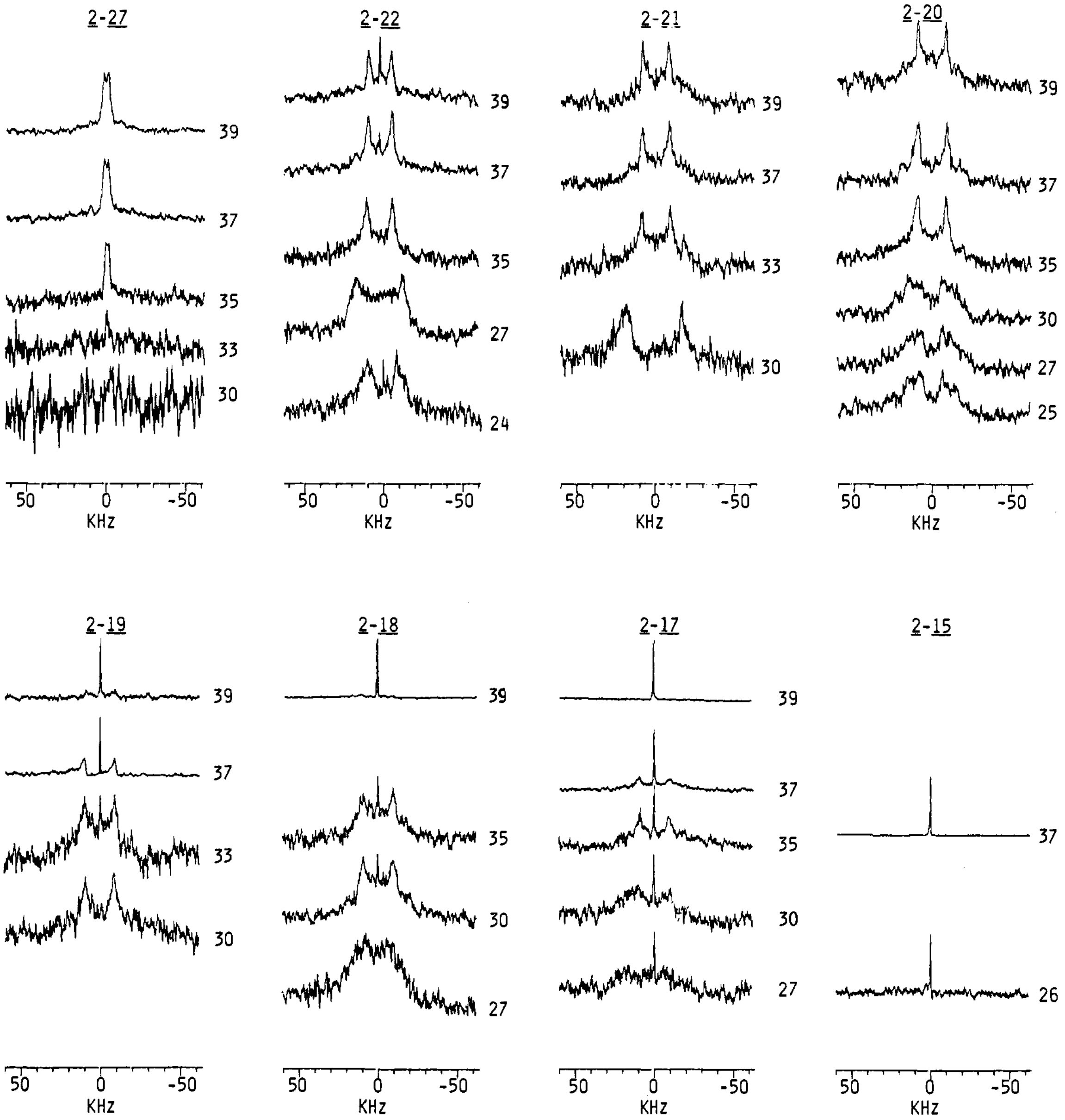

Figure 6. ^{2}H NMR spectra (1-s delay) of 3 wt% α-deuteriated **2-*N*** in **C21** at various temperatures (°C).

The selectivity (S) in the distribution of photoproducts upon their irradiation in solid n-alkane phases (see Tables V and VI) is defined in eq 2 (where p represents a solid phase and i represents

$$S_{ec} = (E/C)_p/(E/C)_i \qquad (2a)$$

$$S_{lc} = (t/c)_p/(t/c)_i \qquad (2b)$$

the isotropic phase of the same n-alkane). These ratios of ratios provide a direct measure of the influence of phase anisotropy of the course of the photochemical reactions: the solvent molecules are invariant in structure in the solid and isotropic phases; only their organization, mobility, and, perhaps, conformation differ.

Discussion

Most of the photochemical studies were conducted with samples of 1 wt% ketone in n-alkanes. Unfortunately our thermal and optical measurements lack the sensitivity to detect perturbation of the n-alkane properties in such dilute samples and corresponding ^{2}H NMR spectra contained unacceptably low signal-to-noise ratios. By extrapolating results from 3 (or more) wt% of ketone, we conclude that samples of 1 wt% of **2-*N*** or ***m*-*N*** ($15 < N < 22$) in **C21** form solid solutions in the nonisotropic temperature range investigated; 1 wt% of alkanones with $23 \leq N \leq 15$ may not, at least at some temperatures.

Not surprisingly, the higher concentration samples in which the most ideal solid solutions form correspond to ketones with N equal to or 1 less than the number of carbon atoms in the n-alkane host. By contrast, ketones do *not* form solutions well if N is even 1 more than the number of carbon atoms in the n-alkane. Examples of aberrant behavior are found in 3 wt% ketone samples consisting of $N = 21$ in **C20**, **2-22** in **C21**, and $N = 27$ in **C26**.

Ketones which are well-incorporated are assumed to be isomorphously substituted in solid n-alkane matrices and to exist in all-trans (extended) conformations. Those which are incorporated with extensive disturbance are conformationally more labile. In fact, the ^{2}H NMR spectra indicate that the $N = 13$ (and perhaps $N = 15$) ketones retain sufficient mobility to appear isotropic-like even in Phase I of **C21**. For reasons which have been discussed in the context of the miscibility of mixtures of solid n-alkane homologs,[14,17,20] it is likely that ketone molecules longer than their host n-alkane must adopt gauche bends if even dilute solid solutions form.

The conformational preferences and mobilities of the alkanones in solid n-alkane matrices have important (and complicated) consequences on both the efficiency and selectivity of the Norrish II processes. Scheme I outlines some of the steps most important to this study. For example, the quantum efficiency for Norrish

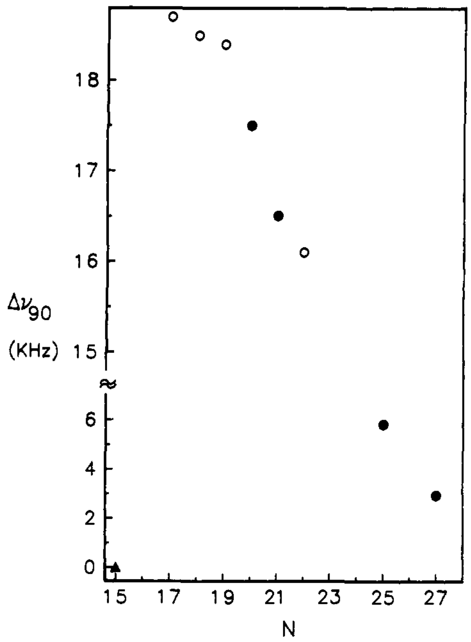

Figure 7. ^{2}H NMR splitting frequencies ($\Delta\gamma_{90}$) versus carbon atom chain length (N) of 3 wt% α-deuteriated **2-*N*** in **C21** at 35 °C: (▲) singlet only; (●) Pake pattern only; (○) Pake pattern and singlet (no data point for singlet).

Scheme I. Representation of the Important Families of Conformers Responsible for Conversion of **2-*N*** and ***m*-*N*** to Their Norrish II Photoproducts

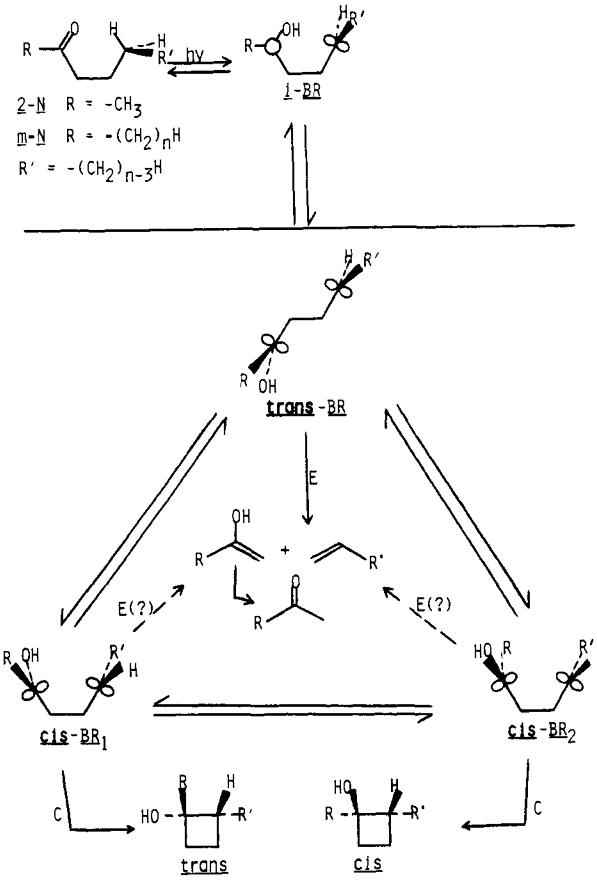

II product formation (Φ) for samples from which the alkanones exist in several frozen or slowly interconverting conformations (with mole fractions χ_i) is $\sum\chi_i\Phi_i$. The ketone molecules with the greatest conformational lability or with a nearly frozen shape which is conducive to formation of *i*-BR and subsequent product formation may skew the observed Φ; the presence of a large mole fraction of unreactive ketone may be masked by a small mole fraction of high reactivity. For these reasons, the data in Tables V and VI must be interpreted with caution.

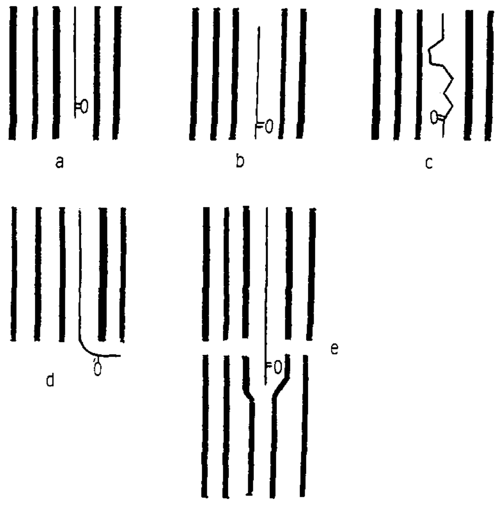

Figure 8. Cartoon representations of possible modes of incorporation of **2-*N*** shorter than **C21** (a and b) and longer than **C21** (c–e) into a solid matrix. The ***m*-*N*** incorporation modes are analogous. The **C21** molecules are depicted as rods and the ketones by lines.

Table V. Norrish II Product Ratios from 1 wt% of **2-*N*** and ***m*-*N*** in **C21**

		2-*N*		*m*-*N*	
N	*T* (°C)	*E*/*C*	*t*/*c*	*E*/*C*	*t*/*c*
13	45	3.1 ± 0.1	1.7 ± 0.1	1.3 ± 0.1	1.4 ± 0.1
	35	2.9 ± 0.1	1.3 ± 0.1	1.4 ± 0.1	1.8 ± 0.1
	25	3.0 ± 0.1	1.1 ± 0.1	1.5 ± 0.1	2.1 ± 0.1
15	45	3.3 ± 0.1	1.8 ± 0.1	1.5 ± 0.1	2.1 ± 0.1
	35	3.7 ± 0.3	1.6 ± 0.1	1.8 ± 0.4	1.8 ± 0.1
	25	16 ± 1	1.6 ± 0.1	2.6 ± 0.1	1.5 ± 0.1
17	45	3.3 ± 0.2	1.7 ± 0.4	1.4 ± 0.1	2.4 ± 0.1
	35	4.6 ± 0.7	3.4 ± 0.2	2.4 ± 0.1	5.9 ± 0.1
	25	15 ± 4	2.4 ± 0.4	5.0 ± 0.9	1.5 ± 0.1
18	45	4.0 ± 0.3	1.5 ± 0.2		
	35	3.9 ± 0.2	4.6 ± 0.2		
	25	14 ± 3	2.4 ± 0.1		
20	45	4.9 ± 0.3	1.6 ± 0.1		
	35	18 ± 4	4.7 ± 0.9		
	25	165 ± 15	18 ± 8		
21	45	2.4 ± 0.1	1.0 ± 0.1	1.8 ± 0.1	2.5 ± 0.1
	35	6.0 ± 2.0	2.5 ± 0.2	3.5 ± 0.1	25 ± 3
	25	46 ± 16	3.6 ± 0.9	>69	0.9 ± 0.4
21[a]	45	2.8 ± 0.1	1.7 ± 0.1	1.4 ± 0.2	1.6 ± 0.5
	35	11 ± 2	1.6 ± 0.1	3.6 ± 0.1	11 ± 1
	25	55 ± 16[b]		40 ± 3	1.6 ± 0.1
22	45	4.0 ± 0.2	1.7 ± 0.2		
	35	8.4 ± 0.5	2.8 ± 0.1		
	25	29 ± 3	4 ± 2		
23	45	3.1 ± 0.7	1.9 ± 0.2	2.0 ± 0.1	2.0 ± 0.2
	35	1.6 ± 0.3	2.4 ± 0.2	2.9 ± 0.1	10.8 ± 0.5
	25	3.6 ± 0.1	3.0 ± 0.1	8.1 ± 0.3	9.0 ± 0.8
25	45			2.3 ± 0.4	2.9 ± 0.3
	35			2.9 ± 0.5	18 ± 1
	25			4.3 ± 0.6	15.0 ± 0.7
27	45	4.0 ± 0.8	1.6 ± 0.1		
	35	3.3 ± 0.2	1.7 ± 0.1	2.8 ± 0.1	27 ± 12
	25	4.4 ± 0.2	1.7 ± 0.2	7 ± 2	12 ± 2
29	45				
	35			3.0 ± 1.0	7.0 ± 0.3
	25			4.4 ± 0.7	8 ± 2
31	45			2.4 ± 0.2	2.1 ± 0.1
	35			2.9 ± 0.4	5.1 ± 0.7
	25			2.8 ± 0.1	8 ± 2

[a] 12 wt%. [b] *t*/*c* could not be calculated due to a solvent impurity at the cis peak. *E*/*C* was calculated assuming *t*/*c* = 1.7.

In isotropic nonviscous solutions, *i*-BR is formed from both the excited singlet and triplet states of *n*-alkanones.[21] Since the ratios

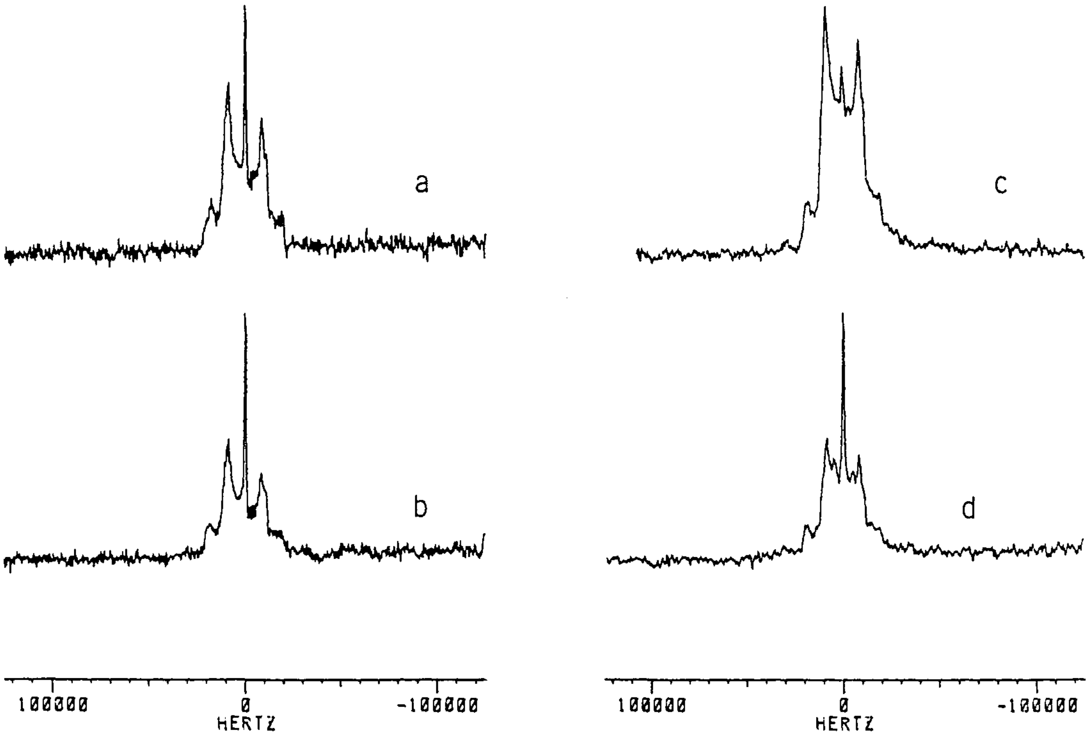

Figure 9. ^{2}H NMR spectra (1-s delay) of **2-17**: (a) neat, 25 °C; (b) neat, 33 °C; (c) 30 wt% in **C21**, 25 °C; (d) 30 wt% in **C21**, 33 °C.

Table VI. Norrish II Product Ratios from Irradiation of 1 wt% **2-*N*** and ***m*-*N*** in **C20** and **C26**[a]

solvent	*N*	*T* (°C)	2-*N* *E*/*C*	2-*N* *t*/*c*	*m*-*N* *E*/*C*	*m*-*N* *t*/*c*
C20	17	42	3.8 ± 0.2	1.8 ± 0.1	1.3 ± 0.1	2.0 ± 0.1
		32	17 ± 4	2.4 ± 0.1	9.0 ± 3.0	1.6 ± 0.3
		25	34 ± 3	4.2 ± 0.5	10.5 ± 0.4	2.3 ± 0.2
C20	19	42	5.5 ± 0.6	1.6 ± 0.1[b]		
		32	210 ± 160	9.0 ± 2[b]		
		25	100 ± 30	11.3 ± 0.6[b]		
C20	20	42	4.0 ± 0.2	2.1 ± 0.8		
		32	66 ± 10	8 ± 6		
		25	69 ± 9	8 ± 6		
C20	21	42	4.7 ± 0.3	1.9 ± 0.1	1.8 ± 0.2	2.4 ± 0.2
		32	4 ± 1	6.8 ± 0.6	7.7 ± 0.4	9 ± 2
		25	5.0 ± 0.7	7.5 ± 0.7	10 ± 2	7.5 ± 0.2
C26	21	60	4.7 ± 0.6	1.5 ± 0.1	1.7 ± 0.1	1.8 ± 0.2
		54	5.7 ± 0.3	3.8 ± 0.1	2.3 ± 0.2	2.8 ± 0.2
		49	12 ± 2	2.1 ± 0.3	5 ± 2	1.3 ± 0.1
		25	27 ± 6	3.1 ± 0.2	13 ± 2	2.6 ± 0.4
C26	27	60	3.0 ± 0.2	1.3 ± 0.2	1.1 ± 0.1[c]	2.9 ± 0.4[c]
		54	7 ± 2[c]	1.9 ± 0.1[c]	3 ± 1[c]	9 ± 2[c]
			7 ± 2	2.4 ± 0.2		
		49	11 ± 4[c]	3.5 ± 0.1[c]	5 ± 2[c]	5.7 ± 0.5[c]
			10 ± 2	9.4 ± 0.9		
		25	39 ± 7[c]	4.4 ± 0.6[c]	7 ± 5[c]	3 ± 1[c]
			15 ± 2	9.1 ± 0.5		

[a] 1 wt% ketone except as noted. [b] ca. 65% conversion of ketone. [c] 3 wt% ketone.

of photoproducts from directly formed *i*-BR^1 are not expected to be the same as those from *i*-BR^3 → *i*-BR^1, the fraction of each ketone excited state which yields *i*-BR *and* the fraction of those intermediates which form products should be known if the *E*/*C* and *t*/*c* ratios in Tables V and VI are to be interpreted reasonably; in isotropic media, directly formed *i*-BR^1 leads primarily to fragmentation products.[22]

Although *trans*-BR can yield only fragmentation products, the families of *cis*-BR can form both cyclization and fragmentation products. In molecules like **2-*N*** and ***m*-*N*** for which internal strain and steric effects are not important, existing evidence indicates that the predominant mode of *cis*-BR reaction is cyclization.[6]

Fortunately, alkanones embedded isomorphously in the organized layers of a solid *n*-alkane should change conformations much more slowly than the rate of intersystem crossing ($\leq 2 \times 10^8$ s^{-1}).[23] In this way, extended, "well-dissolved" alkanones should react predominantly in their triplet manifolds. The absolute quantum efficiencies should be no larger than the triplet yield, <0.6,[24] unless a part of the energy wastage in the singlet manifold is due to a masked chemical process such as the return of some *i*-BR^1 to ketones.

Both Slivinskas and Guillet[25] and we[6a] have found that neat solid ***m*-*N*** are nearly photoinert. Norrish II processes which do occur probably emanate from reaction of molecules at defect sites, and the photoproduct ratios are nonselective.[8] By contrast, neat solid 2-alkanones react slowly to yield photoproducts in moderately selective ratios which depend upon the percent of conversion; at ≤5% conversions, *E*/*C* is typically ≥30.[26] In no cases have the product selectivities from irradiation of neat solid 2-alkanones approached those of isomorphously substituted molecules in solid solutions, like **2-19** or **2-20** in **C20** and **2-20** or **2-21** in Phase I of **C21**.

Very short ketones, due to their nearly isotropic-like behavior in the solid phases of **C20**, **C21**, and **C26**, are expected to undergo reaction as they would in a viscous liquid; products will arise from both the singlet and triplet manifolds, but the triplet part may be of greater importance. Very long ketones, if dissolved in a solid *n*-alkane, may either adopt gauche conformations which favor singlet-state reactions and collapse to products without equili-

---

(21) (a) Encina, M. V.; Lissi, E. A. *J. Photochem.* **1976/1977**, *6*, 173. (b) Encina, M. V.; Nogales, A.; Lissi, E. A. *J. Photochem.* **1975**, *4*, 75. (c) Golemba, F. J.; Guillet, J. E. *Macromolecules* **1972**, *5*, 63.

(22) (a) Yang, N. C.; Elliot, S. P. *J. Am. Chem. Soc.* **1969**, *91*, 7550. (b) Coulson, D. R.; Yang, N. C. *J. Am. Chem. Soc.* **1966**, *88*, 4511. (c) Yang, N. C.; Elliot, S. P.; Kim, B. *J. Am. Chem. Soc.* **1969**, *91*, 7551.

(23) The singlet lifetimes of *n*-alkanones which cannot undergo the Norrish II reactions are reported to be <4.5 ns.[23a] These represent upper limits to singlet lifetimes of alkanones with γ-hydrogen atoms.[23b] (a) Wilkinson, F. *Adv. Photochem.* **1964**, *3*, 255. (b) Dalton, J. C.; Sternfels, R. J. *Mol. Photochem.* **1974**, *6*, 307.

(24) In isotropic hexane solutions at 25 °C, $\Phi(S_1 \rightarrow S_0)$ is reported[22c] to be 0.35 for **2-5** and 0.63 for **2-6**.

(25) Slivinskas, J. A.; Guillet, J. E. *J. Polym. Sci., Polym. Chem. Ed.* **1973**, *11*, 3043.

(26) Weiss, R. G.; Chandrasekhar, S.; Vilalta, P. M. *Collect. Czech. Chem. Commun.*, submitted.

bration of *i*-BR^1 or be forced into conformations which favor triplet-state reactions.

In addition to the aforementioned physical and chemical decay pathways from the excited singlet and triplet states back to the ketone ground state, there exist several other possible modes by which excitation energy may be wasted or ketones consumed without Norrish II product formation. These include Norrish I (α-cleavage)[21,27] and intermolecular hydrogen abstraction (from a neighboring *n*-alkane molecule)[2c] reactions. Due to the constraints imposed upon the migration of the radical pairs from these reactions by solid *n*-alkane matrices, it is reasonable to assume that recombination (energy wasting) is their dominant fate. In support of this contention, we have observed very small amounts of photoproducts not attributable to the Norrish II processes when the conversions are low. If either side reaction were important, Φ_{rel} should have decreased from its isotropic-phase value in both of the solid phases of **C21** for all of the ketones.

Like most other alkanones, our ketones show no detectable phosphorescence in hydrocarbon solutions, indicating that triplet lifetimes are limited by chemical reaction and nonradiative $T_1 \rightarrow S_0$ transitions. We assume that the rates of Type I reactions and nonradiative decay are not highly medium dependent. If these presumptions are correct, there could be a slowing of the rate of the Type II processes by a couple of orders of magnitude before quantum yields are significantly affected. In effect, little information about restriction of motion in the ketone solutes is available from the Φ_{rel} solid-phase data unless they are significantly different from those in isotropic media.

As expected, all of the Φ_{rel} values measured from irradiation of the ***m*-*N*** in isotropic (liquid-phase) **C21** are the same within experimental error. The large increase in Φ_{rel} observed upon irradiation of **7-13** in Phase I of **C21** may be due to the ubiquitous problem of increased light diffraction in the solid phase. DSC and ^{2}H NMR data demonstrate that specific solvation effects by solid **C21** do not control the efficiency of reaction of **7-13**. Only in the most ordered Phase I is a somewhat depressed value of Φ_{rel} observed for **11-21**. The result was not anticipated, since the **11-21** molecules are extended and their reactive carbonyl groups are almost surely held rather firmly in the middle of the hydrocarbon layers in both solid phases.

The very high values of Φ_{rel}, the surprisingly large *t*/*c* cyclobutanol ratios (vide infra), and the observations concerning the conformations of *n*-alkane molecules in solid matrices of their lower homologues[14,17,20] support the suggestion that the very long ketones **14-27** and **16-31** are bent in Phase I of **C21**. If the ketone molecules in that state were chain-extended, as in the neat crystals,[28] Φ_{rel} should be near zero. The fraction which has a gauche twist near the carbonyl group may be able to form *i*-BR quite efficiently from the excited singlet state and collapse to products (or return to ground-state ketone) without equilibrating the *trans*-BR, *cis*-BR$_1$, and *cis*-BR$_2$ structures.[22] In Phase II, the same ketone molecules undergo Norrish II photoreactions with clearly attenuated efficiencies. Although we cannot suggest an attractive explanation for these results, the less-demanding Phase II matrix may permit a larger fraction of the **14-27** and **16-31** molecules to exist in conformations which include no gauche bends near the solute carbonyl groups.

An attractive simplification of the mechanism, which may well be correct at least for alkanones which are no more than 1 carbon atom longer than their alkane hosts, involves the assumptions (1) that virtually all reaction emanates from the triplet manifold, (2) that BR^3 to BR^1 intersystem crossing rates are slower than the rates of BR conformational interconversion, and (3) that the BR^3 to BR^1 rates are about equal in all of the preproduct conformers. In this case, the ratios of photoproducts reflect the relative *stabilities* of the various preproduct BR^3 precursors and not the rates for their interconversion (i.e., an equilibrium among them is established prior to BR$^3 \rightarrow$ BR^1). However, in Phase I or **C21** or at lower temperatures in the solid phases of **C20** and **C26**, BR triplets from isomorphously substituted alkanones within the tight alkane matrices may *not* be able to reach equilibrium populations of conformers prior to intersystem crossing. In these instances, the photoproduct ratios will depend upon the *energy barriers* separating *i*–BR and the preproduct conformers and, to the extent that equilibrium is partially established, the equilibrium constants among the conformers. Clearly, the data in hand allow only tentative mechanistic conclusions to be drawn.

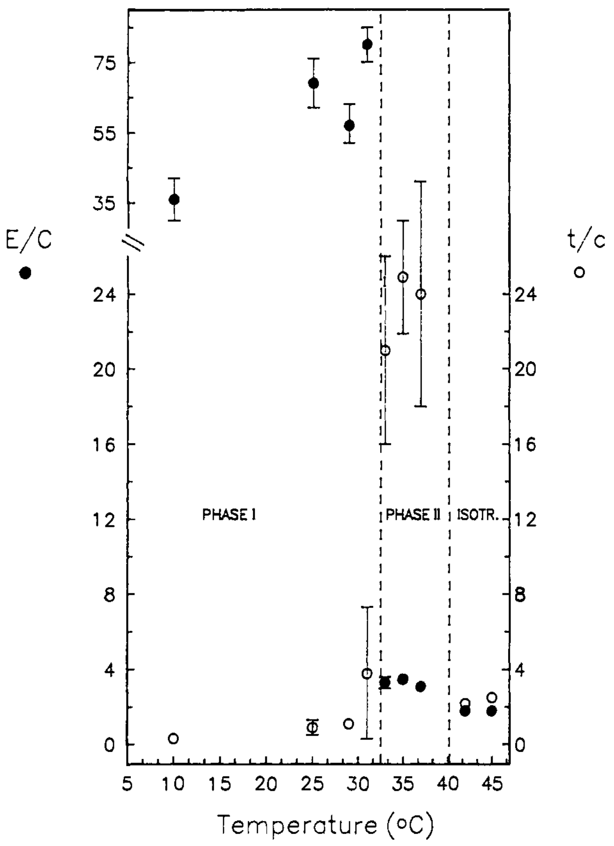

Figure 10. *E*/*C* (●) and *t*/*c* (○) photoproduct ratios from irradiation of 1 wt% of **11-21** in **C21**. Transition temperatures are indicated with dashed lines.

The isomorphously substituted **11-21** ketone at 1 wt% shows a nearly nonselective *E*/*C* ratio in Phase II of **C21** and a very high value (>69 at 25 °C) in Phase I. On the other hand, the S_{1c} vaue is very high (about 10) in Phase II but inverted (about 0.35) in Phase I. Further evidence for isomorphous substitution of **11-21** is found in the selectivities measured upon irradiation of 12 wt% of ketone in **C21** (within the solid solution concentration limits): the S_{cc} and S_{1c} values are similar to those obtained from the 1 wt% solutions, indicating that **11-21** does not disturb greatly the **C21** matrix. If *cis*-BR$_2$ is the most difficult conformer to form in a layered phase and equilibrium among the BRs is established in Phase II, the high *t*/*c* selectivity and relatively low *E*/*C* selectivity are reasonable, since the steric demands of *cis*-BR$_1$ and *trans*-BR from ***m*-*N*** are quite similar. In Phase I, only the *E*/*C* ratio is considered mechanistically important, since less than 2% of the product mixture is cyclobutanols; we reiterate that these cyclobutanols may be formed from ketone molecules at defects in the lattice. The tightness of the cybotactic regions afforded in Phase I may force *i*-BR into its most compatible conformation, *trans*-BR, and result in the very high *E*/*C* ratio. Figure 10 shows that the change from nonselective to very selective *E*/*C* ratios is abrupt and occurs at the Phase I–Phase II transition temperature without further meaningful changes at various temperatures within a phase.

Results from irradiation of **2-21** in **C21** offer an opportunity to examine the restraints imposed by Phase I and Phase II on reactions occurring near a layer boundary. As with **11-21**, the

---

(27) Li, S.-K.; Guillet, J. E. *Polym. Photochem.* **1984**, *4*, 21.

(28) (a) Sullivan, P. K. *J. Res. Natl. Bur. Stand.* **1974**, *78A*, 129. (b) Bailey, A. V.; Mitcham, D.; Skau, E. L. *J. Chem. Eng. Data* **1970**, *15*, 542. (c) Saville, W. B.; Schaerer, G. *J. Chem. Soc.* **1925**, *127*, 591.

1 and 12 wt% ketone samples provide very similar values of S_{ec} and S_{1c} and further evidence for isomorphous substitution by the **2-21** molecules. Since greater disorder occurs near a layer boundary than in the vicinity of a layer middle (where the reaction center of **11-21** molecules is expected to reside), we expected that the S_{ec} and S_{1c} values from the $m = 2$ isomer would be lower than those from the $m = 11$. Although that is the case for t/c ratios in Phase II, the E/C ratios from the two isomers in Phase I are certainly comparable. The lack of selectivity in the t/c ratios from **2-21** may be ascribed primarily to the similarity in the van der Waals volumes of the two substituents on the 2-carbon of the BR, methyl and hydroxyl. The very large S_{ec} values from irradiations of **2-21** in Phase I require that the terminal methyl and adjacent methylene groups of **C21** in Phase I near a **2-21** molecule retain a great deal of order as anticipated by the ^{2}H NMR spectra.

Large values of S_{ec} are also found when 1 wt% of **2-20** is irradiated in the solid phase of **C20**. Although the layering of solid-phase **C20** and **C21** is different, both are able to exert significant control over the motions of the BR whose carbon chain lengths match the alkane. Again, we prefer not to comment upon the t/c ratios from **2-20** in **C20** because the cyclobutanol yields are very small.

Results from alkanones which are 1 carbon atom shorter than the host solvent molecules reveal *greater* selectivity than when the alkanone and hydrocarbon contain equal numbers of carbon atoms. In fact, the E/C ratios from **2-20** in solid **C21** are among the largest we have measured from irradiation of any ordered system, including neat ketone crystals.[26,29] Although our DSC and ^{2}H NMR experiments indicate that solid solutions containing up to 3 wt% of **2-20** are nearly ideal, we anticipated that solvent influence would not be as great in these systems as in those containing **2-21**. This is not the case. In Phase I and Phase II of **C21**, the S_{ec} values from **2-20** follow the trends from **2-21** but are larger. The E/C selectivities from **2-19** and **2-20** in **C20** follow the same trends. The S_{1c} values from **2-20** in **C21** (ca. 11 at 25 °C) and from **2-19** in **C20** (ca. 7 at 25 °C) are probably too large to be dismissed even though the total yield of cyclobutanols in each case is very small. Figure 11 shows that the t/c and E/C ratios from **2-20** are consistent throughout each of the solid phases of **C21** and that the selectivity jump coincides with the phase transition temperatures.

The aforementioned model for shorter **2-*N*** which are nearly isomorphously substituted into the solid *n*-alkane matrices (Figure 8a) predicts that the carbonyl and its nearby methylene groups will be subject to a greater restriction of motion (due to the compression of methylene groups on neighboring *n*-alkane molecules as they attempt to fill the spatial void) and a greater local mobility (due to the increased torsional motion available to methylene groups in the vicinity). The balance between these two factors may determine the magnitudes of the selectivities; that balance appears to be maximized when the alkanones are 1 carbon atom shorter than the hydrocarbon hosts.

Evidence for the disruption created in the *n*-alkane solid lattices by **2-*N*** which are shorter than their hosts is clearly discernible in the DSC experiments and from density measurements performed on *n*-alkane mixtures.[14b] The ^{2}H NMR spectral studies on α-deuteriated **2-17**, **3-17**, and **4-17** in **C21** demonstrate that significant motion of the methylene groups of the ketones persists, at least to the 3-carbon and perhaps to the 5-carbon, even in Phase I.

Thus, **2-19** in **C20** and **2-20** in **C21** are expected to be in a highly ordered, but somewhat malleable, environment. More importantly, neighboring hydrocarbon molecules exert a steric compression upon the carbonyl and adjacent methylene groups of these **2-*N*** which is greater than that experienced by **2-*N*** 1 carbon atom longer. This steric compression must be exerted throughout the sequence of events from excitation of the carbonyl group, formation of the BR, and eventual formation of products. In this way, the BR will be compelled to retain conformations as extended as possible (N.B., *trans*-BR) in order to minimize both the void near the layer boundary and the force exerted by neighboring hydrocarbon molecules. If this model is correct, it predicts that solutes which fit best into an ordered solvent matrix will not always react with the greatest selectivity. Recent examples from this laboratory are consistent with this contention.[29]

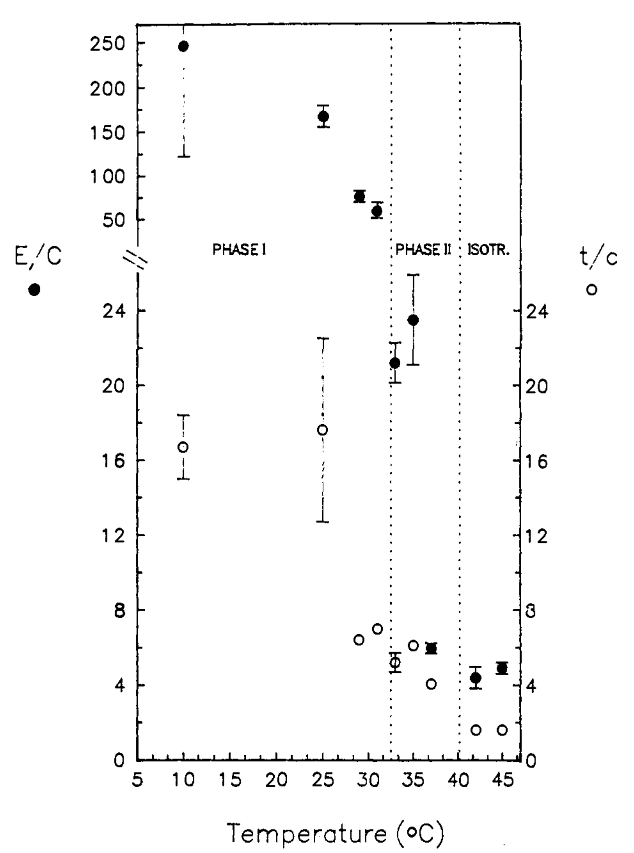

Figure 11. E/C (●) and t/c (○) photoproduct ratios from irradiation of **2-20** in **C21**. The concentration is 1 wt% for all points except 2 wt% for those at 33 and 37 °C. Transition temperatures are indicated with dotted lines.

Ketones containing 1 carbon atom more than their hydrocarbon hosts form very disturbed solid solutions or mixtures at 3 wt% concentrations as judged by our DSC experiments. Also, the ^{2}H NMR spectrum of α-deuteriated **2-22** in solid **C21** clearly indicates that its deuterons are in a less ordered environment than those of **2-21** in the same solvent (Figure 6).

This can be construed as a consequence of the longer guests occupying an excess of the normally allotted molecular volume in the solvent matrix and causing an expansive pressure on it. In contrast, guests whose lengths are one carbon atom shorter than the host molecules create an excess of *free* volume and a negative pressure on the matrix. At 1 wt%, the concentration at which most of the irradiations were performed, the vast majority of the longer alkanone molecules appear to be incorporated into their hydrocarbon solid phases. In all likelihood, a small fraction is in phase-separated environments; although the solid phase-separated ***m*-*N*** are probably less photochemically reactive than the dissolved ketone component, we have no idea about the relative reactivities of incorporated and phase-separated **2-*N***. Irradiation of the solid phases of these ***m*-*N***-containing systems results in E/C and t/c selectivities which are somewhat elevated. Except for **2-21** in **C20**, the E/C ratios from the solid systems containing **2-*N*** are also elevated. Clearly the selectivities are significantly lower than those found from irradiation of the well-incorporated alkanones. They are consistent with the view that none of these

---

(29) (a) Furman, I.; Weiss, R. G. *J. Am. Chem. Soc.* **1992**, *114*, 1391. (b) Furman, I.; Butcher, R. J.; Catchings, R. M.; Weiss, R. G. *J. Am. Chem. Soc.* **1992**, *114*, 6023. (c) Vilalta, P. M.; Hammond, G. S.; Weiss, R. G. *Photochem. Photobiol.* **1991**, *54*, 563. (d) Vilalta, P. M. Ph.D. Thesis, Georgetown University, Washington, DC, 1992.

(30) (a) Weiss, R. G. *Tetrahedron* **1988**, *44*, 3413. (b) Weiss, R. G. In *Photochemistry in Organized and Constrained Media*; Ramamurthy, V., Ed.; VCH Publishers: New York, 1991; Chapter 14.

guests is held rigidly by the hosts.

As discussed previously, it is quite plausible that the acetyl portions of these **2-*N*** reside at ill-defined, somewhat disorganized layer interfaces. The disturbance to local order caused by the need to place an extra methylene unit in the space allocated for a shorter hydrocarbon molecule is probably felt along the total layer length, since **14-27** in **C26** and **11-21** in **C20** do not behave very differently from their 2-isomers.

A survey of the other results reveals no major surprises but does provide a few suggestive clues. There are no examples of E/C ratios as high as those shown by the best fitting pairs. There are a few examples, notably high t/c ratios, always accompanied by values of E/C not much greater than those observed in isotropic media. In several instances, t/c decreased and E/C increased when an intermediate temperature was decreased to the lowest in a series. These facts are consistent with the view that the motions differentiating the formation of trans and cis cyclobutanols are the first level of sensitivity to environmental steric constraints. As such, they should be manifested in the t/c ratios primarily from those systems in which either the activation barriers for BR interconversion preclude an equilibration prior to intersystem crossing or the ground-state conformations of the alkanones are conducive to γ-hydrogen abstraction from excited singlet states (and subsequent rapid collapse of the BR singlets to products prior to their equilibration). These ketones are expected to be the ones which are longer than their hydrocarbon host.

Irradiation of 1 wt% of the $N = 17$ ketones does not show any striking anomaly in their product distributions; the results are those expected of a solid solution in which the ketone does not fit very well in the host matrix. The E/C ratio of 15 ± 4 for **2-17** at 25 °C indicates considerable restriction of configuration in the solid solution. Irradiations were also conducted at 30 wt% of the $N = 17$ ketones in **C21** (near the eutectic composition). To minimize surface photochemistry in these cases, the radiation was filtered through a Corning 0-54 filter (10% transmittance at 313 nm). No selectivity in the photoproduct ratios from either of the heptadecanone isomers can be discerned: both E/C and t/c remain at 1.5–3 for irradiations conducted between 45 and 20 °C. Since ^{2}H NMR results indicate that the eutectic mixture consists of microcrystallites of ketone (plus a small fraction dissolved in **C21**) and **C21**, no selectivity was expected from the **9-17** irradiations. The absence of selectivity from irradiation of the **2-17/C21** eutectic may be due to the acetyl groups being exposed, on average, to an environment which differs from that in the neat solid. For instance, the **2-17** microcrystallite boundaries with **C21** may be rather disordered.

The substantial selectivity of the E/C ratio found upon irradiation of **2-15** (as compared with **2-13**) in Phase I of **C21** indicates that an additional two methylene units allows ca. 1 wt% of ketone to be incorporated into the alkane layers. However, the isotropic-like ^{2}H NMR spectrum of α-deuteriated **2-15** at 3 wt% concentration in Phase I of **C21** demonstrates that these ketone molecules must reside in a highly disturbed environment; the solid solutions are far from ideal.

Comparison with Results from Irradiations in Other Ordered Layered Phases. As can be seen, the selectivities from Norrish II product ratios depend on a complex convolution of factors which include solvent order and mobility, the solubility of the alkanones in the medium, the local disturbance created by the alkanone to its local environment, the specific location of the carbonyl group within the alkanone, and the multiplicity of the reactive excited state. In spite of this complexity, several clear trends have been identified and the results from most of the experiments can be placed logically into a part of a more global scheme.

Previously, we have examined the Norrish II reactions of **2-*N*** and ***m*-*N*** in the other layered phases in which several of the complications identified above (such as solubility) are not important. These phases include the hexatic B and solid phases of *n*-butyl stearate (BS),[5,6] the interdigitated bilayer gel phase of 50% aqueous potassium stearate (KS), and the bilayer gel phase of 50% aqueous 1/1 1-octadecanol/potassium stearate (KSO).[6c,7,8] Details concerning the modes of fragmentation and cyclization of the alkanones in these phases have been discussed previously.[30] Since each of these phases is less ordered but more malleable than the solid *n*-alkane phases employed here, it is useful to compare the magnitudes of the selectivities in each and the range of the alkanone homologues over which the selectivity is manifested. Our most complete body of data in the solid phases of **C21** will be compared in this context. Due to the probable domination of the modes of reaction of the BRs from 2-alkanones in KS and KSO by hydrogen bonding,[7] data from the system will not be included here.

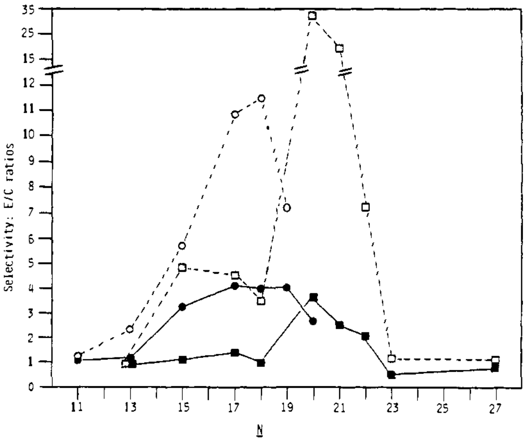

Figure 12. E/C selectivities from irradiation of **2-*N*** in BS (●, ○) and in **C21** (■, □): (●) from 20 °C/30 °C data; (○) from 0 °C/30 °C data; (■) from 35 °C/45 °C data; (□) from 25 °C/45 °C data.

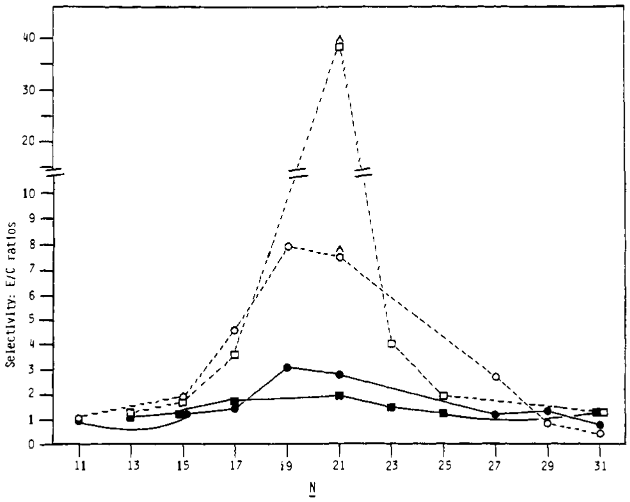

Figure 13. E/C selectivities from irradiation of ***m*-*N*** in BS (●, ○) and in **C21** (■, □). Symbols as described in Figure 12 legend. Carats indicate lower limits to selectivities.

Figures 12 and 13 present a pictoral view of the dependence of S_{ec} ratios on the carbon atom length of **2-*N*** and ***m*-*N*** in the various phases. The data points should be considered in relationship to the length of the respective solvent molecules: in terms of lengths analogous to N, we take these to be 17 for KS and KSO, 23 for *n*-BS, and 21 for C21. For greater clarity, the points of each phase have been connected in spite of the fact that not all homologues are represented. Data for ***m*-*N*** in KS and KSO are also excluded for clarity and because the selectivities of the E/C ratios in these systems are virtually invariant over a wide range of solute lengths.[7]

It can be seen from the figures that reactions in Phase I of **C21** provide the largest values of S_{ec}, but over a narrower range of alkanone homologues than in any of the other ordered phases. Thus, although the conditions under which the solvent order of Phase I exerts control on the behavior of a reactive solute are the most stringent, the magnitude of their influence on the affected solutes is also the greatest. Essentially, this very stiff, well-ordered phase accepts solutes into or rejects them from its crystal structure more critically than do the more malleable ordered phases. The latter can accommodate a wider range of solute shapes and sizes due to their own lower intermolecular ordering. However, once in one of the malleable matrices, even the best-fit solutes experience an environment which is more tolerant of conformational change.

Also, we have noted previously that irradiation of neat solid *n*-alkanones does not result in photoproduct selectivity which is as great as that found when the same ketones are dissolved in solid solutions of *n*-alkanes with the same number of carbon atoms. Thus, the greatest restriction to motion experienced by an alkanone molecule is not always that afforded by its crystalline matrix nor is it presented by more malleable liquid-crystalline environments. We believe that this conclusion should apply to the reactions of many other solutes.

Acknowledgment. We thank the National Science Foundation for its support of this work and Dr. Patricia Vilalta for helpful discussions. A.N. acknowledges the Consejo Nacional de Investigaciones Cientificas y Tecnicas de la Republica de la Argentina for a travel grant.

Electron-Transfer Oxidation of Ketene Silyl Acetals and Other Organosilanes. The Mechanistic Insight into Lewis Acid Mediated Electron Transfer

Shunichi Fukuzumi,[*,†] Morifumi Fujita,[†] Junzo Otera,[*,‡] and Yukihiro Fujita[‡]

Contribution from the Department of Applied Chemistry, Faculty of Engineering, Osaka University, Suita, Osaka 565, Japan, and Department of Applied Chemistry, Okayama University of Science, Ridai-cho, Okayama 700, Japan. *Received April 27, 1992*

Abstract: Kinetic studies on photoinduced and thermal electron-transfer oxidation of a variety of organosilanes in acetonitrile at 298 K are reported in terms of the electron-transfer rate constants (k_{et}) with a series of oxidants having the known one-electron reduction potentials (E^0_{red}). The Rehm–Weller Gibbs energy relationship is applied to determine the fundamental parameters for the electron-transfer oxidation, i.e., the one-electron oxidation potentials (E^0_{ox}) and the intrinsic barrier for the electron-transfer oxidation ($\Delta G^{\ddagger}_0$). The E^0_{ox} and $\Delta G^{\ddagger}_0$ values thus obtained are compared with the calculated values of the adiabatic ionization potentials (I_a) and the inner-sphere reorganization energies (λ_i) associated with the structural change upon electron-transfer oxidation by using the PM3 molecular orbital method. Ketene silyl acetals, especially hindered ones, are shown to act as unique and strong electron donors as compared to other organosilanes. On the other hand, Lewis acids such as $SnCl_4$, Ph_3SiClO_4, and Et_3SiClO_4, which catalyze the addition of hindered ketene acetals to α-enones, are shown to act as strong electron acceptors in the electron-transfer oxidation of ferrocene derivatives. The mechanistic insight to the electron-transfer oxidation of organosilanes, particularly in the case of hindered ketene silyl acetals which are employed in Lewis acid promoted carbon–carbon bond formation reactions, is discussed on the basis of the fundamental parameters for the electron-transfer oxidation.

Introduction

Organosilanes have been frequently used as key reagents for many synthetically important transformations. Lewis acid promoted carbon–carbon bond formation reactions of organosilanes such as allylsilanes, enol silyl ethers, and ketene silyl acetals expecially have been of considerable interest in organic synthesis in recent years.[1] Quantitative information on the reactivities of allylsilanes and enol silyl ethers acting as nucleophiles has recently been derived from the kinetic investigations on the reactions of diarylcarbenium ions with these important organosilanes.[2] On the other hand, electron-transfer oxidation of organosilanes has also been receiving increased attention recently in both thermal[3,4] and photochemical[5–7] reactions. However, the fundamental properties such as the one-electron oxidation potentials (E^0_{ox}) and the intrinsic barrier for the electron-transfer oxidation of organosilanes have, to the best of our knowledge, not yet been available.

We report herein the kinetic investigations on both the photoinduced and thermal electron-transfer oxidation of various organosilanes to determine the E^0_{ox} and $\Delta G^{\ddagger}_0$ values that would otherwise be difficult to obtain.[8] The E^0_{ox} and $\Delta G^{\ddagger}_0$ values thus obtained are compared with those predicted by the molecular orbital calculations. In addition, we determined the rate constants of the electron-transfer reduction of some Lewis acids that are frequently used as promoters for the C–C bond formation reactions. These data provide the energetic basis for the Lewis acid mediated electron-transfer processes of organosilanes as well as

---

[†] Osaka University.

[‡] Okayama University of Science.

(1) (a) Colvin, E. W. *Silicon in Organic Synthesis*; Butterworths: London, 1981. (b) Mukaiyama, T. *Angew. Chem., Int. Ed. Engl.* **1977**, *16*, 817. (c) Mukaiyama, T.; Murakami, M. *Synthesis* **1987**, 1043. (d) Gennari, C. *Selectivities in Lewis Acid Promoted Reactions*; Schinzer, D., Ed.; Kluwer Academic Publishers: Dordrecht, The Netherlands, 1989; Chapter 4, p 53. (e) Heathcock, C. H. *Aldrichimica Acta* **1990**, *23*, 99.

(2) (a) Bartl, J.; Steenken, S.; Mayr, H. *J. Am. Chem. Soc.* **1991**, *113*, 7710. (b) Hagen, G.; Mayr, H. *J. Am. Chem. Soc.* **1991**, *113*, 4954. (c) Mary, H. *Angew. Chem., Int. Ed. Engl.* **1990**, *29*, 1371.

(3) (a) Reetz, M. T.; Schwellnus, K.; Hübner, F.; Massa, W.; Schmidt, R. E. *Chem. Ber.* **1983**, *116*, 3708. (b) Baciocchi, E.; Casu, A.; Ruzziconi, R. *Tetrahedron Lett.* **1989**, *30*, 3707. (c) Snider, R. B.; Kwon, T. *J. Org. Chem.* **1990**, *55*, 4786. (d) Ali, S. M.; Rousseau, G. *Tetrahedron* **1990**, *46*, 7011. (e) Totten, C. E.; Wenke, G.; Karydas, A. C.; Rhodes, Y. E. *Synth. Commun.* **1985**, *15*, 301. (f) Bhattacharya, A.; DiMichele, L. M.; Dolling, U.-H.; Grabowski, E. J. J.; Grenda, V. J. *J. Org. Chem.* **1989**, *54*, 6118. (g) Yoshida, J.; Maekawa, T.; Murata, T.; Matsunaga, S.; Isoe, S. *J. Am. Chem. Soc.* **1990**, *112*, 1962. (h) Fukuzumi, S.; Kitano, T.; Mochida, K. *J. Am. Chem. Soc.* **1990**, *112*, 3246.

(4) A number of stable organosilicon radical cations have been reported: Kaim, W. *Acc. Chem. Res.* **1985**, *18*, 160 and references cited therein.

(5) Mariano, P. S. *Photoinduced Electron Transfer*; Fox, M. A., Chanon, M., Eds.; Elsevier: Amsterdam, 1988; Part C, p 372 and references cited therein.

(6) (a) Gassman, P. G.; Hay, B. A. *J. Am. Chem. Soc.* **1986**, *108*, 4227. (b) Gassman, P. G.; Hay, B. A. *J. Am. Chem. Soc.* **1985**, *107*, 4075. (c) Gassman, P. G.; Bottorff, K. J. *J. Org. Chem.* **1988**, *53*, 1097. (d) Dinnocenzo, J. P.; Farid, S.; Goodman, J. L.; Gould, I. R.; Todd, W. P.; Mattes, S. L. *J. Am. Chem. Soc.* **1989**, *111*, 8973.

0002-7863/92/1514-10271$03.00/0